New Jersey Institute of Technology

Digital Commons @ NJIT

8-31-1990

Design of a microengineered pressure sensor

Ranjeet Alexis
New Jersey Institute of Technology

Follow this and additional works at: https://digitalcommons.njit.edu/theses

Part of the Electrical and Electronics Commons

Recommended Citation

DESIGN OF A
MICROENGINEERED PRESSURE SENSOR

by

Ranjeet Alexis

APPROVAL SHEET

Title of Thesis: Design of a
                          Microengineered Vacuum Pressure Sensor

Name of Candidate: Ranjeet Alexis
                          Master of Science in Electrical Engineering, 1989

Thesis and Abstract Approved:

June 18, 1989

Dr. William N. Carr   Date
Professor

Jne 19, 89

Dr. Durga Misra   Date
Assistant Professor

Date 6·19·89

Dr. N.M. Ravindra   Date
Assistant Professor

VITA

Name: Ranjeet Alexis

Permanent address:

Degree and date to be conferred: M.S.E.E., October 1989.

Date of birth:

Place of birth:

Secondary Education: Don Bosco Higher Secondary School, Madras, India.

Collegiate Institutions Attended:

Name	Date	Degree	Date of Degree
New Jersey Institute of Technology, NJ	Jan. 1988 to May. 1989	MSEE	October 1989
College of Engineering Annamalai Univ., India	Aug. 1982 to June 1986	BSEE	June 1986

Major: Electrical Engineering.

ABSTRACT

Design of a Microengineered Pressure Sensor.

(June 1989)

Ranjeet Alexis, M.S.E.E., New Jersey Institute of Technology

Thesis Advisor: Dr. William N. Carr

A new family of microengineered vacuum ionization gauges of an approximate volume of $200\mu^3$ has been designed. These devices can be fabricated using existing semiconductor processing capabilities. The focus of this thesis is to scale down the current state-of-the-art for ionization sensors to micron dimensions. These gauges can be manufactured economically and potentially will be integrated with more complex structures and circuitry. In these devices an active ionization volume of micron dimensions is used for launching ions in a trajectory towards a collection electrode. Ionization of gas species is accomplished by an electron flux of sufficient energy. Analysis of electron and ion ballistics was carried out using SIMION, an interactive workstation based simulator. Two different ionization processes have been simulated. The first one is called avalanche ionization in which a B field is incorporated into the device. In the second case, ionization is accomplished using field emission sources of electrons. The collection electrode is positioned in planer structures for high efficiency collection of ions of interest. A family of geometries are simulated and optimized for compatability with semiconductor processing and operational efficiency. Devices based on 3 and 4 photolithographic masking levels are described in this thesis. The maximum pressure ambient for this family of devices is limited by sputtering of electrodes. The minimum detectable pressure level of 10^{-7}torr is determined by electrometer sensitivities and device current leakage.

W. N. C.

6/22/89

ACKNOWLEDGMENTS

TABLE OF CONTENTS

LIST OF FIGURES

CHAPTER I

INTRODUCTION

The main focus of this thesis was to design a microengineeered pressure gauge that could operate with stability and give out accurate indications of the pressure inside a chamber. The pressure range over which this device could operate is between 10^{-4} torr to 10^{-7} torr.

This thesis is organized into five parts.The first part chapter 2 describes the basic transport process in a gas, kinetics of thermal motion, elastic and inelastic collisions. Also discussed in this chapter are other areas like ionization, mean free path and atomic cross-sections. This serves as the foundation on which the subsequent chapters were researched and written. Chapter 3, discusses the existing vacuum gauges and their principle of operation. A number of illustrations, figures for each of these gauges have been included.

In chapter 4, a device geometry that is able to measure pressure using the Avalanche ionization technique has been discussed. In this device, an electron is subjected to the influence of an electric and magnetic field. It's path is tremendously increased, since it is engaged in a helical motion. This electron ionizes any molecules in its path which in the process produces more electrons. These electrons continue to ionize other molecules and this continues like a chain reaction until all the molecules in the active

1

volume are ionized. The resulting ionization current is then collected and when measured gives us an indication of the pressure inside the chamber. Fabrication steps are suggested. Included in this chapter are the simulation results from SIMION which show the electron and ion trajectories.

In chapter 5, another device, also used to measure pressure but using a different principle has been discussed. In this device, the pressure is measured by collecting the ionization current. But this ionization is different from Avalanche ionization in the sense that the electrons are not subject to any magnetic field. A large number of electrons are produced by means of field emission. These electrons strike the ambient gas molecules thereby ionizing them.

The Fowler-Nordheim phenomena as related to field emission has also been discussed.

CHAPTER II

FUNDAMENTAL OF IDEAL GASES.

2-1 Kinetic Theory Of Ideal Gases

Many problems in the study of rarified gases can be conveniently tackled if we use the concept of an ideal gas. An ideal gas is assumed to have a number of specific properties, namely:

- its molecules can be treated as point masses;

-its molecules exert no force on one another or on the walls of the container, expect when they collide;

- the distance of separate between the molecules are very large when compared to their atomic dimensions;

When rarified real gases with which vacuum technology is mostly concerned come very close to ideal gases as regards to their properties, as long as their temperatures are not close to liquefaction point and their pressures are not too high.

2-2 Thermal Effects On Molecules and Atoms

In any solid, liquid or gaseous substance its molecules are in random motion. This is called thermal motion and is the basis for the kinetic theory of matter.

3

In a solid , the thermal motion of its particles are oscillatory about a mean position at various amplitudes. In fact, they can not move in any other way, as they are held together by strong bonds (forces of mutual attraction). Hence a solid can retain its volume and shape. In a liquid, the molecules move about in a mixed fashion, that is , they both oscillate and move in straight (or rather, zigzag) paths. As the temperature of a liquid rises, the zigzag motion becomes increasingly more predominant, because the molecules can overcome mutual attraction more easily. Accordingly, a liquid can retain on its own accord only its volume, but not its shape. In a gas, the molecules move (or tend to move) in straight lines only, the interaction between them is negligible. So gases are incapable of retaining their shape or volume. Hence a gas will always expand tending to occupy all the available volume.

Understanding the thermal motion of molecules can help us to understand most of the events that fall within the domain of vacuum engineering. Some of them are:-

- Random thermal motion which stands behind the ability of gases to expand and take up all of the available volume and penetrate into one another (also termed as diffusion).

- Thermal conduction, which is the transport of heat from a hotter to a cooler gaseous medium.

- The thermal motion of molecules which contributes to some of the inter-

nal energy inherent in any substance .

In a real gas,the total internal energy is the sum of the kinetic energy due to the thermal motion of molecules and the potential energy due to their interaction. The potential energy builds up with increasing mean distance between the molecules which is the same, as decrease in pressure.

In an ideal gas, since the molecules do not exert any force on each other; hence the internal energy is only the kinetic energy due to the thermal motion. Hence we may conclude that in an ideal gas, at a given pressure the gas molecules have a certain definite velocity.

2-3 Velocity and Speed Of Gas Molecules

The molecules in a gas are in thermal motion, at all possible velocities which differ in both magnitude and direction. The velocities of the molecules in a gas may be characterised by mean velocity of the molecules which is the velocity of a molecule measured over a long period of time or the velocities of all the molecules measured at that particular instant. As given by Maxwell, a gas not subjected to any external, mechanical or temperature influence would always settle to a state in which its molecules would be distributed in velocity by the Maxwell's distribution law . Using this law we can calculate the most probable speed, that is ,frequently encountered among gas molecules. The Maxwell's distribution law, states

that for a given speed v

$$\frac{1}{n} \equiv f_v = \frac{4}{\sqrt{\pi}} [\frac{m}{2kT}]^{\frac{3}{2}} v^2 exp[-\frac{mv^2}{2kT}] \qquad (.1)$$

where m is the mass of a molecule. this equation states that if there are n

molecules in the volume, there will be dn molecules having a speed between

v and $v + dv$. The average speed is obtainable from Eq. 1.1

$$v_{av} = \frac{\int_0^\infty v f_v dv}{\int_0^\infty f_v dv} = \frac{2}{\sqrt{\pi}} \sqrt{\frac{2kT}{m}} \qquad (.2)$$

Graphically the velocity distribution is shown in Fig. 2.1, plotted for two

fixed temperatures ($T_2 > T_1$). In the plot, it has been assumed that the total

number of molecules represented by the area bounded by the curve and the

x-axis is the same in both cases. As seen the rise in temperature, shifts the

curve towards higher velocities.
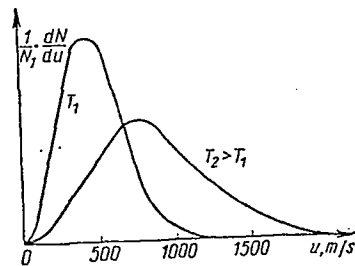
Fig 2.1 Velocity distribution of
gas molecules (1/N) (dN/du) is the
concentration of molecules having
a given velocity u, m s^{-1} (Ref 14)

6

2-4 Mean Free Path

The molecules due to thermal energy, move in a random fashion. During the random motion they collide with other molecules. Between collisions, the molecules travel in straight lines. At collisions they change direction, so on the whole they move in a zigzag fashion. The minimum distance travelled by a molecule between two successive collisions is called the mean free path. The minimum time elapsed between two successive collision is called mean free time. A molecule having a diameter d and velocity v will move a distance $v\delta t$ in time δt. The molecule suffers from a collision with another molecule if its center is anywhere within the distance d of the center of another molecule. Therefore; it sweeps out (without collisions) a cylinder of diameter $2d$. The volume of the cylinder is given by

$$\delta V = \pi/4 (2d)^2 v \delta t \tag{.3}$$

Since there are n molecules$/cm^3$,the volume associated with one molecule is on the average $\frac{1}{n} cm^3$. When the volume δ is equal to $\frac{1}{n}$ it must contain on the average one other molecule; thus, a collision has occurred. If $\tau = \delta t$ is the average time between collisions, then we have

$$1/n = \pi d^2 v \tau \tag{.4}$$

and the mean free path λ is then

$$\lambda = v\tau = 1/\pi n d^2 \tag{.5}$$

7

The ideal gas law states that

$$PV = RT = N_{avo}KT \qquad (.6)$$

where P is the pressure, V is the volume of one molr gas , R is the gas constant (1.98 cal/mol-K,or 82 atm-cm^3/mol-K), T is the absolute temperature in K, N_{avo} is the Avogrado's constant (6.023×10^{23}molecules/mol) and k, is the Boltzman constant(1.38×10^{-23}J/K).

Since real gases behave more and more like the ideal gas as the pressure is lowered, Eq(.6) is valid for most vacuum processes. Using this equation we can calculate the molecular concentration (the number of molecules per unit volume) given by

$$n = N_{avo}/V = P/KT$$

end From Eq(.3) and Eq(.4) we can now say that

$$\lambda = \frac{KT}{\pi P d^2} \qquad (.9)$$

For air molecules at room temperature where the equivalent molecular diameter is $3.7 A^0$ the dependence of mean free path and pressure is given by

$$\lambda = \frac{5 \times 10^{-3}}{P(in Torr)} \qquad (.10)$$

This can be investigated in greater detail. We know that a molecule moving with a velocity U_{rel} with respect to other molecules will sweep out

in one second a volume $(\pi/4)d^2 U_{rel}$. Since the number of molecules per unit volume is N_1, the number of collisions one molecule can make per unit volume is $\pi\sigma^2 U_{rel} N_1$. Hence, the mean free path is

$$\lambda = U_a/\pi\sigma U_{rel} N \qquad (.11)$$
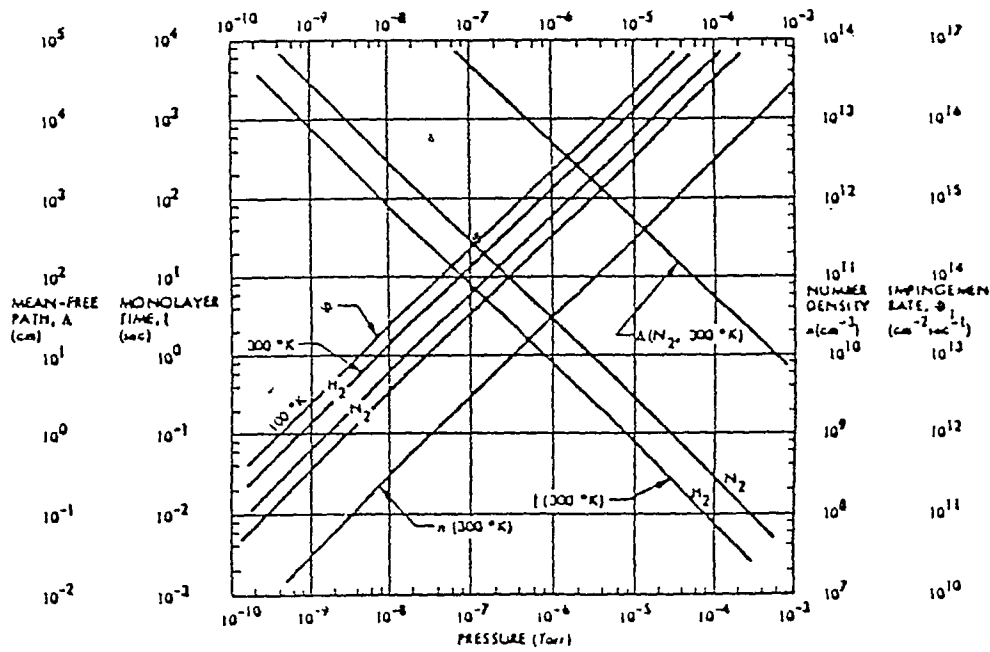
Dependence of mean free path on pressure.
(Ref. Journal of Vacuum Science Tech. 4, 139, 1967)

Fig 2.2

The two molecules involved in a collision are both moving. Therefore, on assuming that they are moving at the same speed, we obtain by the cosine law

$$U_{rel} = \sqrt{U_a^2 + U_a^2 - 2U_a^2 Cos\theta} \qquad (.12)$$

where θ is the angle between the velocity vectors of the molecules. Since θ can take on positive and negative values with the same probability we may write

$$2U_a^2 cos\theta = 0 \qquad (.13)$$

Then

$$\lambda = 1/\sqrt{2}\ N_1 \pi d2 \qquad (.14)$$

In deriving Eq(.5), it was assumed that the apparent diameter d remained constant with variations in temperature. To account for the effect of temperature on the apparent diameter, an experimental correction factor is applied to the above equation. Then,

$$\lambda = 1/\sqrt{2}N_1 \pi \sigma^2 (1 + C/T) \qquad (.15)$$

where C is a constant dependent on the kind of gas involved and T is the temperature in Kelvins. The value of C for hydrogen, helium, air, oxygen and argon are 84.4, 80, 112, 125 and 142 repectively.

If we denote the mean free path of a molecule at 273K as λ_{273} and at any other temperature as λ_T,then using Eq.15 we can find that

$$\lambda_T = \lambda_{273}\frac{(273 + C')T}{(T + C')273} \qquad (.16)$$

10

2-5 Transport Processes in a Gas

Transport processes take place in nonequilibrium systems. Of special interest are those processes which finally drive an originally non equilibrium system to an equilibrium state.

With regard to a confined gas, a non equilibrium state refers to some difference or gradient in the gas. Thermal motion tends to equalize such differences or gradients. If this causes mass transfer, we speak of diffusion. Momentum transfer is referred to as viscosity. Energy or heat transfer has to do with heat(or thermal) conduction.

Let the momentum, mass or energy be distributed in a nonuniform fashion. Let "f" represent any one of these quantities. Suppose that f is nonuniformly distributed solely along the Z axis and its distribution in planes parallel to the XY plane is uniform. Then we may say that f is solely a function of the Z coordinate. It is to be noted that the transport variable f will proceed differently in different direction. It will be a maximum in the Z direction which is at right angles to the XY plane. Obviously, the greater the difference in the transport variable between two points, the larger its transport. It is usual to consider the transport of f along the normal to the surface of zero gradient, that is, the XY plane.

Let us choose two arbitrary parallel planes with coordinates Z_1 and Z_2 spaced Z apart. Suppose that in the Z_1 plane the transport variable is f(Z_1) and in the Z_2 plane it is f(Z_2). Then the transport between the two

planes in the Z direction will be

$$f = k_f \frac{f(Z_2) - f(Z_1)}{Z} A \tag{.17}$$

or with Z tending to zero,

$$f = k_f \frac{d[f(Z)]}{dZ} A \tag{.18}$$

where k_f is the coefficient taking care of the number and kind of molecules taking part in the transport process.

d[f(Z)]/dZ is the gradient in the transport variable transferred by one molecule.

A is the surface area through which transport occurs.

Considering the transport process from the view point of kinetic energy we see that the number of molecules that cross a unit area per unit time in the Z direction is $N_1 U_a / 6$. The molecules that reach without collision at Z are only those which are at a distance equal to the mean free path on either sides of that. In other words, these will be molecules at planes with coordinates $(Z+\lambda)$ and $(Z-\lambda)$. Accordingly, the change in the transport variable at the specified plane will be $f(Z+\lambda) - f(Z-\lambda)$.

Let $f(Z+\lambda)$ and $f(Z-\lambda)$ be expanded into power series and let us retain only the first term in each series. Then,

$$f = (Z + \lambda) = f(Z) + \lambda \frac{d[f(Z)]}{dZ} \tag{.19}$$

12

and

$$f = (Z - \lambda) = f(Z) - \lambda \frac{d[f(Z)]}{dZ} \qquad (.20)$$

Then the change in f at the chosen plane will be

$$f(Z + \lambda) - f(Z - \lambda) = 2\lambda \frac{d[f(Z)]}{dZ} \qquad (.21)$$

Hence, the total value of the f transport variable transferred across an area A per unit time will be

$$f = \frac{1}{6} N_1 U_a \times 2\lambda \frac{d[f(Z)]}{dZ} A = \frac{1}{3} U_a \lambda \frac{d[N_1 f(Z)]}{dZ} A \qquad (.22)$$

2-6 Ionization Current The pressure in a chamber containing a certain amount of gas is nothing but a number which gives us an indication of the total number of molecules in that chamber. Since all these molecules at room temperature have thermal energy they move about randomly. However, if we consider a small volume (say 1 cubic micron) within this chamber, the total number of molecules in this volume will remain the same if observed over a long period of time.

From the ideal gas laws we know that the total number of molecules per unit volume is given by

$$Number - of - molecules/unitvolume = \frac{P}{kT} \qquad (.23)$$

Assuming three degrees of freedom the velocity of the molecules is given by

$$v = \sqrt{\frac{3kT}{M}} \qquad (.24)$$

13

Since each molecule has an equal probability of moving in the X,Y or Z direction the total number of molecules crossing the XY plane is given by

$$\frac{1}{3}[\frac{P}{kT}]\sqrt{\frac{3kT}{M}}A^2 \tag{.25}$$

where A^2 is the area of the plane. From the above equation we may conclude that the total number of molecules crossing any imaginary surface within the chamber depends on the pressure inside the chamber.

If we are able to ionize all of these molecules that cross this imaginary plane, and then collect these ionized atoms(ions) then the ionization current that results, gives us an indication of the pressure within the chamber. The ionization current for various pressures at constant volume and the ionization current for various volumes at constant pressure are shown fig 2.3 a and fig 2.3 b. Thus we see that higher the pressure and larger the volume greater the ionization that takes place.

Fig 2.3a

15

Fig 2.3b

16
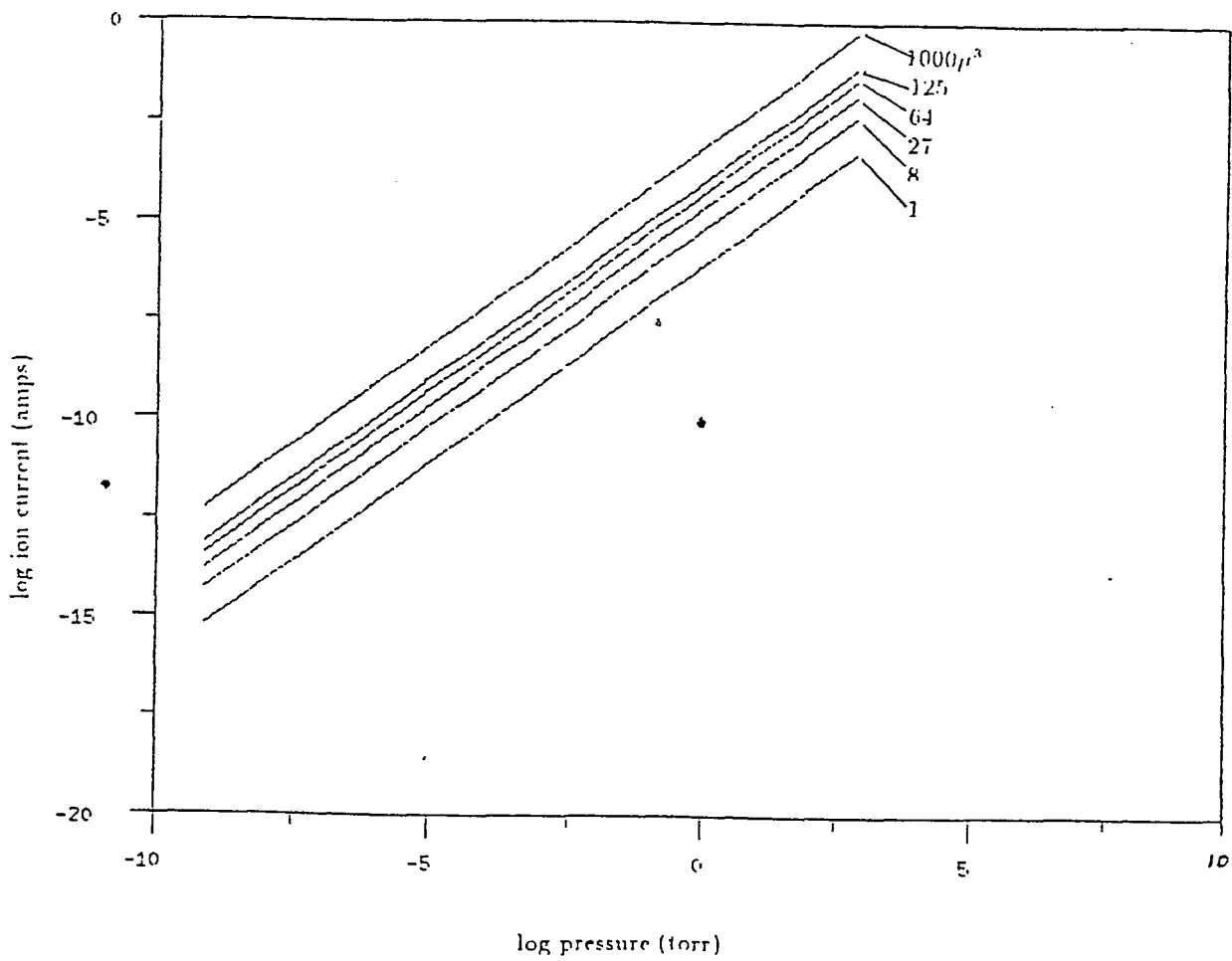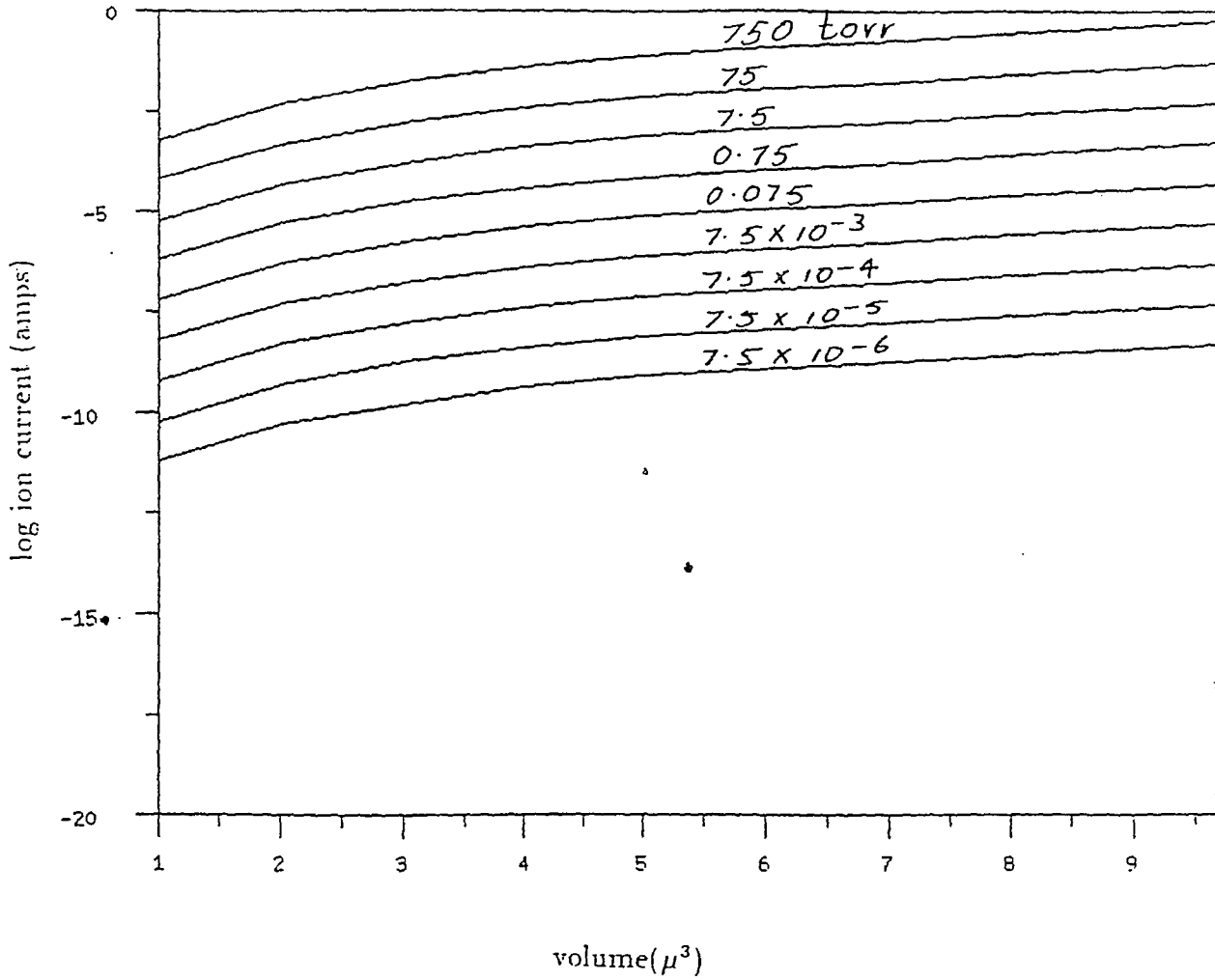
2-7 Elastic and Inelastic Collisions

Collision processes can be broadly divided into elastic and inelastic types, according to whether the internal energies of the colliding bodies are maintained. Particles usually have two types of energies namely kinetic and potential energy. Kinetic energy is due to their motion and is equal to $\frac{1}{2}mv^2$. The potential or internal energy which may be in the form of electronic excitation, ionization etc.

An elastic collision is one in which there is an interchange of kinetic energy only. An inelastic collision has no such restriction and internal energies also change. Consider two bodies of masses m_i and m_t which suffer an elastic binary collision. Assume that m_t is initially stationary and that m_i collides with velocity v_i at an angle θ to the line joining the centers of m_i and m_t at the moment of collision. By the law of conservation of linear momentum

$$m_i v_i cos\theta = m_i u_i + m_t u_t \qquad (.26)$$

By the law of conservation of energy

$$\frac{1}{2}m_i v_i^2 = \frac{1}{2}m_i(u_i^2 + v_i^2 sin_2\theta) + \frac{1}{2}m_t u_t^2 \qquad (.27)$$

Eliminating u_i in Eq(.2) from Eq(.1) gives

$$m_i v_i^2 cos_2\theta = \frac{m_i}{m_t^2}(m_i v_i cos\theta - m_t u_t)_2 + m_t u_t^2 \qquad (.28)$$

The fractional energy transferred from mass m_i to m_t is

$$\frac{E_t}{E_i} = \frac{\frac{1}{2}m_t u_t^2}{\frac{1}{2}m_i v_i^2} = \frac{4m_i m_t}{(m_i + m_t)^2}cos^2\theta \qquad (.29)$$

17

and this has a maximum of $\cos^2\theta$ when $m_i = m_t$. As a consequence, the fraction of energy transferred from an electron to a nitrogen molecule was about 10^{-4}. But if we now allow the collision to be inelastic, so that the molecules struck gain internal energy of δu, we can again determine the fraction of energy transferred, by using the same equations used previously

Momentum conservation

$$m_i v_i cos\theta = m_i u_i + m_t u_t \qquad (.30)$$

Energy conservation

$$\frac{1}{2}m_i v_i^2 = \frac{1}{2}m_i(u_i^2 + v_i^2 sin_2\theta) + \frac{1}{2}m_t u_t^2 + \Delta u \qquad (.$$

Eliminating u_i as before and simplifying gives

$$2m_t u_t v_i cos\theta = \frac{m_t}{m_i}(m_t + m_i)u_t^2 + 2\Delta u \qquad (.32)$$

Δu and u_t are the only variables. To maximize Δu

$$2\frac{d}{du_t}\delta u = 2m_t v_i cos\theta - \frac{m_t}{m_i}(m_t + m_i)2u_t = 0 \qquad (.33)$$

or

$$v_i cos\theta = \frac{(m_t + m_i)}{m_i}u_t \qquad (.34)$$

Hence we have

$$2\Delta u = (\frac{m_t m_i}{m_t + m_i})v_i^2 cos^2\theta \qquad (.35)$$

18

Hence the fraction of the kinetic energy of the first particle that can be transferred to the internal energy of the second, has a minimum value of

$$\frac{\Delta u}{\frac{1}{2}m_i v_i^2} = \frac{m_t}{m_t + m_i}\cos^2\theta \qquad (.36)$$

So where as the minimum elastic energy transfer from an electron to a nitrogen molecule was only 0.01 percent by inelastic means this may rise to more than 99.99 percent, since when $m_t >> m_i$, this inelastic energy transfer function tends to 1.

From the above discussion, we can calculate the fractional kinetic energy transfer, which is

$$\frac{\frac{1}{2}m_t u_t^2}{\frac{1}{2}m_i v_i^2} = \frac{m_t u_t^2}{m_i}\left(\frac{2m_t u_t}{\frac{m_t}{m_i}(m_t + m_i)u_i^2 + 2\Delta u}\right)^2$$

Excluding the cases when Δu can be negative, this function has a maximum value when the denominator has a minium value given by $\Delta u = 0$; then the fractional energy transfer will become equal to

$$4\frac{m_i m_t}{(m_i + m_t)^2} \qquad (.38)$$

as expected. So, even though a good deal of potential energy can be transferred when $m_i << m_t$, it is still impossible to transfer any significant amount of kinetic energy.

19

2-8 Ionization

All other types of electron collisions are inelastic. The most important of these is the electron impact ionization.fig.2.4.

Electron impact ionization
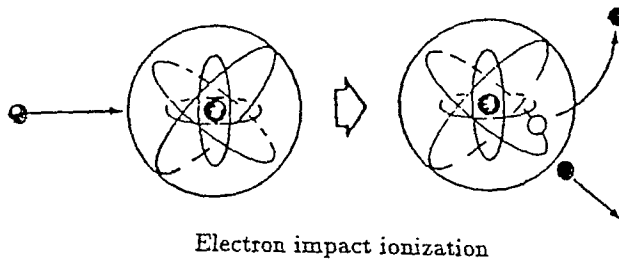
Fig 2.4

In this case the primary electron removes an electron from the atom, producing a positive ion and two electrons, e.g.

$$e + Ar \rightarrow 2e + Ar^+ \qquad (.39)$$

The two electrons produced by the ionizing collisions can then be accelerated by an electric field until they too can produce ionization. It is by this multiplication process that complete ionization is achieved. There is a minimum energy requirement for this ionization. Process to occur, equal to the energy to remove the weakly bound electron from the atom, and this is known as ionization potential; for Xenon this has a minimum value of

12.08eV. Below this threshold energy, the ionization cross-section is clearly zero, but rises as soon as the electron exceeds the ionization potential fig (2.5).
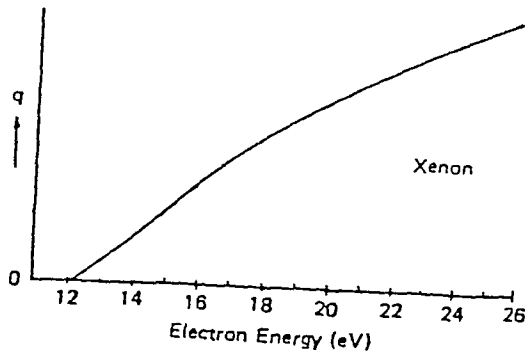
Ionization cross-section for xenon near threshold (Rapp and Englander-Golden 1965)

Fig 2.5

The energy dependence on the ionization cross-section for xenon over a rather larger electron energy range is shown in Fig(2.6).

This is fairly typical of the inert gases, quickly rising above the threshold to a maximum around 100eV and then falling. Cross-sections for other noble gases are shown in Fig(2.7). Note that this figure gives the cross-sections in units of πa_0^2 rather than cm_2. In this unit, a_0 is the radius (0.53×10^{-8}) of the first Bohr orbit of hydrogen. πa_0^2 is the area of the hydrogen atom and has the value $8.82 \times 10^{-17} cm^2$, a unit of useful size.

21
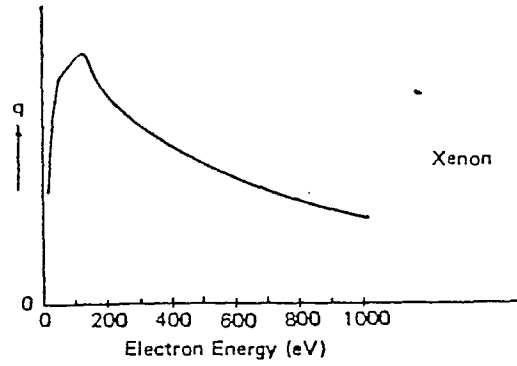
Ionization cross-section for xenon, 0-1000 eV (Rapp and Englander-Golden 1965)

Fig 2.6
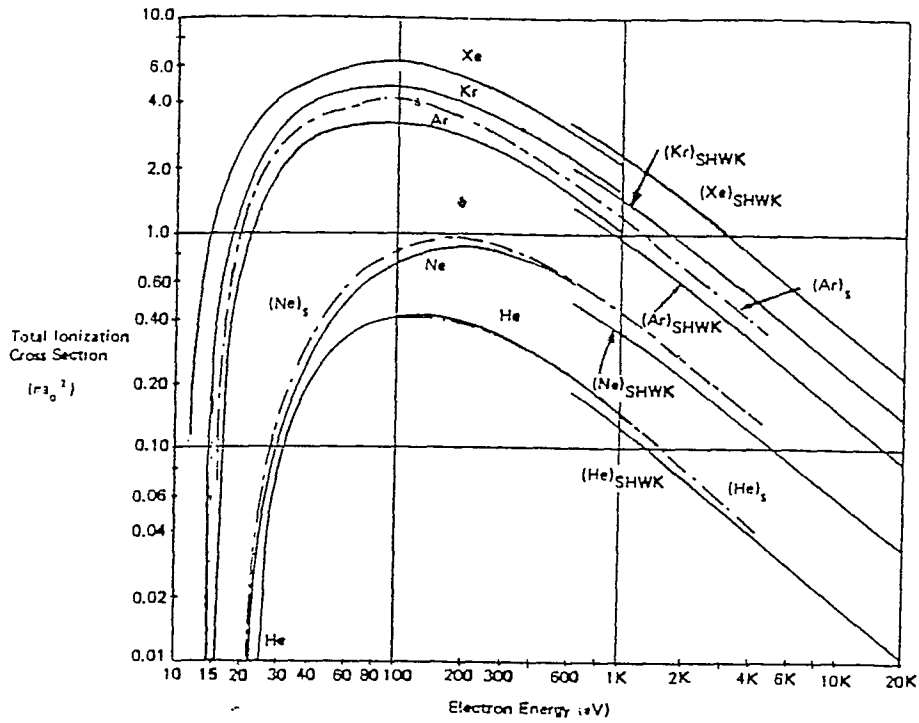
Ionization cross-sections of the noble gases (from Rapp and Englander-Golden 1965; includes data from (S) Smith 1930 and (SHWK) Schram et al. 1965. Similar values for Ar, He and Ne have been obtained by Fletcher and Cowling 1973); n.b. $\pi a_0^2 = 8.82 \times 10^{-17}$ cm^2

Fig 2.7

CHAPTER III

VACUUM GAUGES

3.1 CLASSIFICATION

A vacuum gauge refers to an instrument designed to measure pressures below atmospheric. Typically, a vacuum gauge is a remote indicating instrument which consists of a gauge proper and a measuring (or control) unit or circuit.

With reference to rarefied gases the concept of pressure is practically meaningless. In vacuum work, processes involving force per unit area(which is the true definition of pressure) are almost non existent. Instead, one is interested in the mass density ρ,of a gaseous medium, and its molecular (or number) density N_1.

The molecular density of a gas is a major factor in heat transfer, absorption and desorption, interaction with structural elements in a vacuum device, and other events occurring in a vacuum.

The pressure 'p' and the molecular density N_1 of a gas are connected by a relation of the form

$$p/N_1 = kT \qquad (.1)$$

In SI units, the pressure of rarefied gases is measured in pascals (Pa). Conversion to other units of pressure and relation to molecular density are given in Table 3.1.

According to principles of operation, vacuum gauges may be classified as follows.

Pressure Units and Molecular Density of Gases at 293 K

Unit	Pa (N/m^2)	mm Hg (torr)	at	bar	$N_1,\ m^{-3}$
Pascal	1	0.75×10^{-2}	0.99×10^{-5}	1.00×10^{-5}	2.47×10^{20}
mm Hg (torr)	133.32	1	1.32×10^{-3}	1.33×10^{-3}	3.29×10^{22}
at (technical atmosphere)	1.01×10^5	760	1	1.01	2.50×10^{25}
bar	1.00×10^5	750	0.99	1	2.47×10^{25}

(1) Liquid-level vacuum gauges (such as U-tube units and their modifications) which measure vacuum directly.

(2) Hydrostatic-pressure gauges which depend for their operation on isothermal compression of an ideal gas (the McLeod gauge).

(3) Mechanical vacuum gauges which use bellows, a Burdon tube or some other elastic deformable element as a sensor and in which the deformation of elastic element is a measure of the vacuum.

(4) Thermal conductivity vacuum gauges which utilize dependence of the thermal conductivity of gases on pressure . They may be built around a

thermocouple or a high -resistance wire .

(5) Ionization vacuum gauges which utilize, as their name implies, the ionization of gases. They may be further sub divide into

(a) hot-cathode (or thermionic) ionization gauges in which electrons produced by a hot filament are accelerated by an electric field .

(b) cold cathode ionization gauges which utilize a glow discharge in electric and magnetic fields (the Penning discharge) to increase the path-length of electrons.

The respective pressure ranges are listed in Fig.3.1. A further classification of all vacuum gauges is into direct-reading (or absolute) and inferential (or indirect).

As the name implies, the former reads the pressures of a gas directly. Their calibration (response to pressure) can be calculated from their geometry or established against a dynamometric instrument. In principle, they read actually for all gases, whatever their composition or temperature. The pressure range extends from 1×10^5 to 1×10^{-3}Pa. Their accuracy improves with rising pressure. Examples of direct reading instruments are liquid level, McLeod and mechanical vacuum gauges.

Inferential do not measure pressure as such. Instead, they determine some quantity which is a function of pressure. As a rule, an inferential vacuum gauge consists of a manometer as the sensor and a measuring unit as the display element. Indications (the output signal) of a inferential vacuum

25

gauges do depend on the composition and temperature of the gas involved. The pressure range covered extends from atmospheric to 10^{-10} Pa. Examples are thermal conductivity and ionization gauges
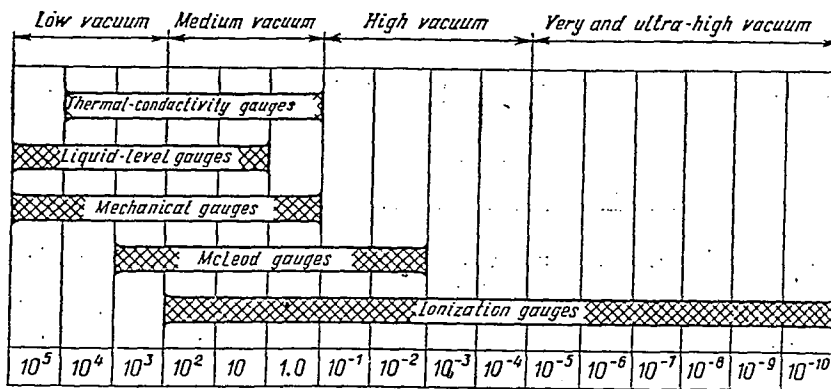
Fig 3.1 Ranges of vacuum gauges

For use as indicating instruments, ionization gauges are fitted with a wide-angle, nearly log rthimic scale. In non indicating application, the

output signal is generated in analog form as a voltage of 0 to 10V which can drive a load of no less than 2 k Ω. This signal can drive a recorder or a controller or fed into a computer.

Frequently, ionization vacuum gauges are ganged up with interlock relays and the combination can then operate as a pressure controller.The interlocking action is set to occur at two points (two values of pressure), so false response is fully prevented. The operating points can be at any spacing, up to the entire range of the vacuum gauge. The relay contacts are designed to interrupt a power of not more than 50 W in d.c. circuits loaded into an inductive load of 2H,and 500 W in a.c. circuits. In the case of circuits carrying heavier currents, the interlocking relay of a vacuum gauge can be used as a pilot relay for a large power relay.

Of all vacuum-gauges types, those most commonly used in the industry are mechanical vacuum gauges and all types of inferential gauges and all types of inferential gauges which are practically free from time lag, cover a wide pressure range, and are simple to handle and maintain.

3.2 U TUBE VACUUM GAUGES

U-tube vacuum gauges measure absolute pressure from atmospheric down to 1 Pa.

The U-tube usually of glass, is partially filled with some liquid (ordinarily, mercury). One arm of the tube to the vacuum to be measured and the

other is sealed off or left open to the atmosphere. The difference in the height between liquid in the two arms give the degree of vacuum in the adopted units (most frequently, in mm of Hg).

OPEN ENDED U-TUBE VACUUM GAUGES

Prior to a pump-down, the pressure above the liquid in two arms is the same (and equal to atmospheric) so the liquid height is also the same. When the pump-down begins,the height of liquid in two arms is different (fig.3.2). The pressure differential p_a-p_x is balanced by the hydrostatic pressure exerted by the difference in height between the two arms.The pressure of the liquid column is given by its mass divided by its cross sectional area and solely depends on the height 'h' and density ρ of the liquid:

$$\Delta p = p_a - p_x = g\rho h \qquad (.2)$$

where

p_a =atmospheric pressure

p_x =unknown pressure

ρ =density of the liquid filling the gauge

h =difference in liquid height between two arms

g =acceleration due to gravity

It is readily seen that indications of an open ended U-tube vacuum gauge depend on the atmospheric pressure. If the atmospheric pressure at the time of measurement is known, it is an easy matter to calculate the absolute

28

pressure in the vacuum system:

$$p_x = p_a - g\rho h \tag{.3}$$

When mercury is used as filling liquid,then

$$p_x = p_a - 1.33 \times 10^2 hPa \tag{.4}$$

where p_a is in pascals and h is in millimeters.

to sum up, in order to measure the pressure in a vacuum system with an open ended U-tube vacuum gauge, it is essential to know the atmospheric pressure at the time of measurement and to substract 1.33×10^2 h from it.
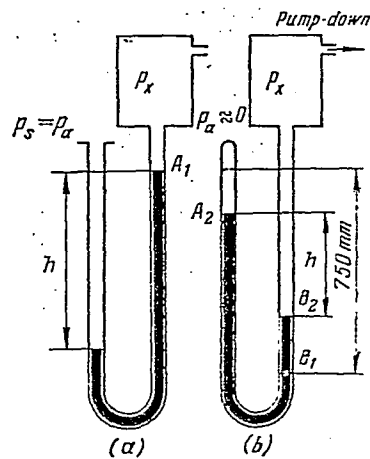
Fig 3.2 U-tube vacuum gauges
a—open-ended; b—closed-ended (Ref. 14)

SEALED-OFF U TUBE VACUUM GAUGES

These measure the difference in pressure between the vacuum system p_x and the sealed-off arm p_s. The filling liquid is mercury which is poured into the gauge already evacuated to a pressure of not over 0.1 Pa. Therefore, the pressure in the sealed off arm $p - s$, may be set equal to zero irrespective of the liquid height in that arm (Torricellian vacuum).

Before the pump-down begins, the pressure in the pumped system is equal to atmospheric, $p_x = p_a$, say, $10^5 Pa$, the mercury takes up position A_1 in the sealed off arm, and the position B_1 on the vacuum side ref fig.3.2b. Obviously, the difference in liquid height $A_1 - B_1$, must be exactly 750 mm, because the difference in pressure in both arms will be balanced in that case.

As the system is pumped down, its pressures decreases, and a smaller difference A_2-B_2 in height between the two arms is now needed to balance the pressure. When the pumped system has been evacuated to a sufficiently low pressure, the height of mercury in the two arms is the same, because the pressure on the vacuum side is now equal to that above the mercury in the sealed-off arm.

To sum up, a sealed-off U-tube vacuum gauge reads the pressure in the pumped system p_x directly as the difference in the liquid height between

the two arms:

$$p_x = 1.33 \times 10^2 h Pa \qquad (.5)$$

where h=A - B is in millimetres.

3.3 HYDROSTATIC PRESSURE VACUUM GAUGES

The most important among these instruments is the Mcleod gauge. This is the only truly absolute gauge for use in the vacuum measurement below 1Pa (0.01mm Hg). Developed by McLeod in 1874, it still remains the backbone of vacuum measurement against which all other gauges are calibrated. One form of the McLeod gauge is shown in fig.3.3. It consists of a glass bulb 1 and a measuring capillary 2 sealed off at top end .Extending downward from the bulb is a tube 3 with a branch 4 connecting the vacuum gauge via another tube 8 to the vacuum to tube 8 to the vacuum gauge to be measured. In turn, tube4 divides to form a reference (or comparison) capillary 5.
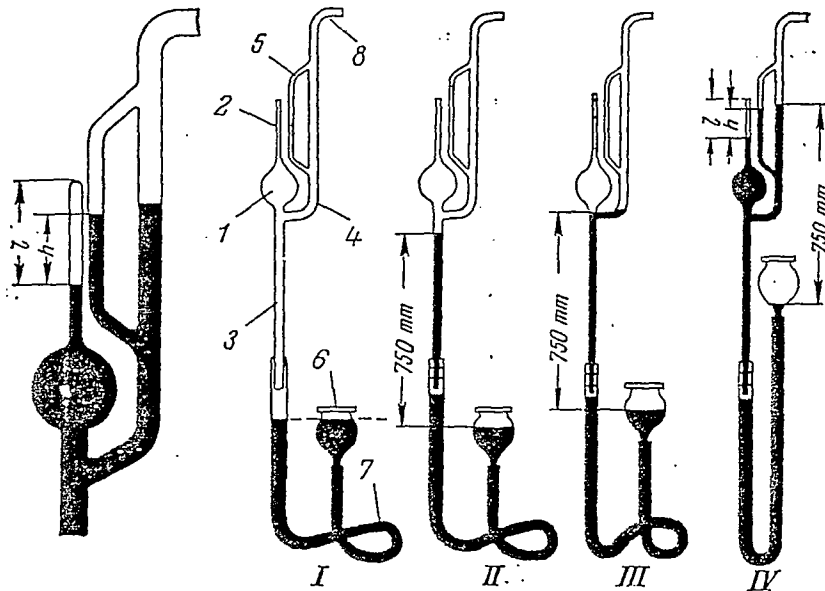
Fig 3.3 Mcleod gauge (Ref. 14)

The two capillaries are usually made of equal bore so as to make up for the capillary depression which acts as source of error. The lower end of the tube 3 is connected by rubber hose 7 to a mercury-filled reservoir 6 The reservoir is open at the top, so the pressure above the mercury level is always equal to atmospheric.

Prior to a measurement, when the pumped system is under atmospheric pressure, the mercury in the reservoir and the rubber hose takes up the same level (see fig. 3.3-i). As the pumped system is exhausted, the mercury level in the rubber hose and also in the tube 3 rises and that in the reservoir falls. When the difference in level attains a value corresponding to the atmospheric pressure (say,750mm Hg) the mercury ceases changing,and the vacuum gauge is ready to measure the pressure in the pumped system (see fig. 3.3-ii). The reservoir and the capillaries must be positioned so that prior to a measurement,the rising mercury could not reach branch 4. Otherwise, mercury would cut off the gauge from the pumped system, and the pressure in the gauge and the system would be different prior to the measurement. To make the measurement,the observer lifts the reservoir . As a result, the mercury tube rises and some time later, cuts off the gauge from the pumped system (see fig.3.3-iii). Now the gauge has trapped a certain quantity of gas p V_1, taking up a volume V_1 which is the sum of the volume of the measuring capillary, the bulb,and the small portion of the tube between bulb and the branch . Obviously, the pressure in the cut off portion is the

same as the pressure in the pumped system p_x.

As the mercury reservoir is lifted still higher, the trapped gas is compressed its pressure rises and its volume decreases in the same proportion.

Suppose that the observer stops lifting the mercury reservoir at the instant when the mercury in the measuring capillary has taken up a certain level (see fig 3.3-4). In the reference capillary the mercury level will higher than it is in the measuring one by height h, because the pressure above the mercury in the reference capillary is lower and equal to p_x.
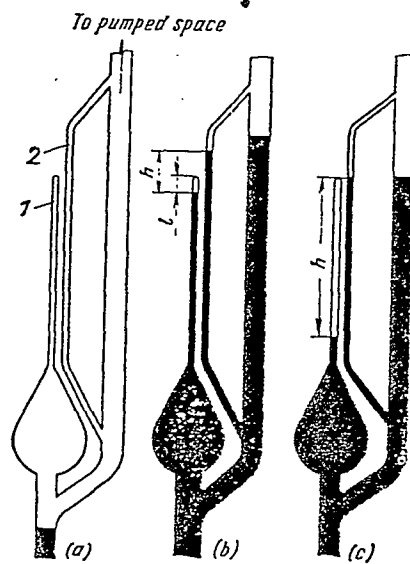
Head of a mecury Mcleod gauge (Ref.14)

a—prior to measurement; b—measurement by the linear scale method; c—measurement by the quadratic (square law) scale method

Fig 3.4

Obviously, the pressure (in mm Hg) of the compressed gas in the measuring capillary is h + P_x,and the quantity of gas compressed is $[h = p_x] \times V_2$. Since quantity of the gas trapped at instant shown in the fig 3.3-iii remains unchanged and the temperature does not practically vary, we may write by Boyle's law

$$p_x V_1 = [h + p_x]V_2 = p \qquad (.6)$$

As a rule McLeod gauge are used to measure low pressure which will not markedly affect the difference in the level h, or which is the same, when $p_x <$ h. Therefore, we may write

$$p_x = 1.33 \times 10^2 (V_2/V_1)hPa \qquad (.7)$$

where h is in millimeters.

To sum up, in order to measure the pressure in a pumped system with a McLeod gauge the intial volume of gas V_1,should be compressed to volume V_2 such that the initial low pressure to be measured p_x is raised to a pressure which can be read directly from the difference in the mercury level h between the measuring and the reference capillaries.

Methods of calibration and measurement.

McLeod gauges can be used calibrated by the linear scale method and the quadratic, or square scale method.

In calibration by the linear scale method the gas is compressed to a known

34

volume (fig.3.3b)labelled with a index mark at height l on capillary 1.The

gas pressure p_1(in mm Hg) in the measuring capillary is of course equal to

the height h of the mercury column in reference capillary 2, as read above

the index mark. The unknown pressure p_x, can be found by

$$p_x = 1.33 \times 10^2 (V_2/V_1)h = k_g \qquad (.8)$$

where

p_x=unknown pressure ,Pa

h=height of the mercury in the reference capillary ,mm

V_1=volume of the bulb and the measuring capillary

V_2= volume of the measuring capillary not filled with mercury

k_g=gauge constant

For a given index mark, k_g has a constant value. Therefore, p_x is directly

proportional to h, the difference in liquid height.

To sum up, the calibration of a McLeod gauge by the linear scale method

reduces to determining the volume left unfilled in the measuring capillary,

V_2, and the total volume V_1, which includes bulb and measuring capillary.It

is an easy matter to see that

$$k_g = 1.33 \times 10^2 (V_2/V_1) = 1.33 \times 10^2 (\pi d^2 l/4V_1) \qquad (.9)$$

In consequence, so as to make the gauge more sensitive to low pressures,

the bulb should have as large a volume V_1, as practicable and the capillary

should have as small bore d, as possible. Conversely, to enable a McLeod gauge to measure higher pressures, the bulb should be small and the capillary should have a large bore.

When a McLeod gauge is calibrated by the square scale method (fig 3.4-C), mercury in the reference capillary is brought up to a level even with the top of the measuring capillary. Then the unknown pressure is given by

$$p_x = 1.33 \times 10^2 (V_2/V_1)h = 1.33 \times 10^2 (\pi d^2 h / 4V_1) h Pa \qquad (.10)$$

where

d= bore of the measuring capillary, mm

V_1= volume of the bulb and measuring capillary,mm

h= mercury height, mm

The term $1.33 \times 10^2 (\pi d^2 h / 4V_1)$,which solely depends on the gauge dimensions, is constant for a given instrument. On denoting it as k_g, we obtain

$$p - x = k_g h^2 \qquad (.11)$$

Since k_g is a constant, the unknown pressure p_x, is directly proportional to the square of the difference in height between the mercury in the measuring and the reference capillaries. This is the reason why this form of calibration is called the square scale method.

Remarks on the McLeod gauge.

Like the U- tube the liquid level gauge, the McLeod gauge is specific

36

in several aspects. This should be borne in mind so as to avoid errors in measuring pressure.

(1) During a measurement, mercury vapour might find its way into the pumped vessel or system and raise the pressure in it.

(2) Because of the manipulations involved, the McLeod gauge cannot read continuously and it is difficult to arrange for remote indication and the use in automatic control systems.

(3) Like the U-tube liquid -level gauges, the McLeod gauge is an absolute vacuum gauge which implies that it can be designed and calibrated with any other vacuum gauge.

3.4 MECHANICAL VACUUM GAUGES

These gauges measure pressure from the atmospheric down to 0.1 Pa. A measure of the unknown pressure is the deformation of an elastic element in response to a change in the pressure difference applied.

A major advantage of a mechanical vacuum gauges is that their indications are independant of the kind of gas involved.

In the laboratories and in the industry, the types more commonly used are the Bourdon -tube vacuum gauge, the diaphragm vacuum gauge, and the capsule (or bellows) vacuum gauges.

BOURDON -TUBE VACUUM GAUGES

In this type of gauge, the sensing element is a curved or twisted (spiral or helical) tube (at 1 in fig. 3.5) other than circular in cross section. One end of the tube is connected to the pumped system via a union 4, and the other is close and coupled by a linkage to a toothed sector 3 which actuates a pointer 2 moving over a scale. On the outside, the Bourdon tube is exposed to the atmospheric pressure at all times. So long as the pressure inside the tube is the same as it is outside (the pressure difference is zerɔ),the tube undergoes no deformation, and the pointer reads zero.
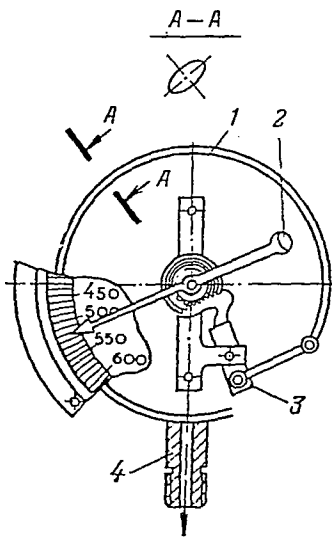
(Ref.14) Bourdon-tube vacuum gauge

1—Bourdon tube; *2*—pointer; *3*—toothed sector; *4*—connection

Fig 3.5
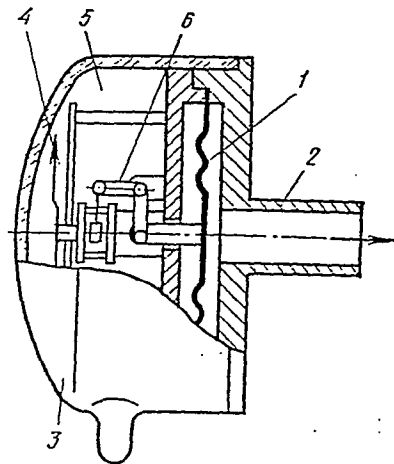
(Ref.14) Diaphragm vacuum gauge

1—diaphragm; *2*—connection; *3*—case; *4*—pointer; *5*—vacuum-tight space evacuated to 0.1 Pa; *6*—lever

Fig 3.6

A change in the pressure in the pumped vessel or system to which the gauge is connected causes the pressure difference to change too, and this brings about a change in the shape (deformation) of the Bourdon tube . The tube tends to become more circular in cross section, and this results in a motion of the closed (or free) end of the tube (tip travel) and, via the linkage and the toothed sector, of the pointer over the scale. The angle through which the pointer moves is proportional to the pressure difference being measured. Obviously, the scale marking, h, against which the pointer stops gives the difference between the atmospheric and the unknown internal pressure p_a-p_x. The unknown pressure is in fact that existing in the pumped system ,so

$$p_x = p_a - h \qquad\qquad (.12)$$

As seen, indications of a Bourdon-tube vacuum gauge depend on atmospheric pressure.

THE DIAPHRAGM VACUUM GAUGES

As in the Bourdon-tube type, a measure of the unknown pressure is given by the deformation of an elastic element which is a diaphragm in this case(fig 3.6) .

The diaphragm 1 forms a vacuum tight space 5 bounded by the case 3 and evacuated to a pressure p< 0.1 Pa (the reference pressure). This space

39

is separated from the pumped vessel to which the gauge is connected by means of a tube union. For the gauge involved the reference pressure may be deemed equal to zero, so the difference in the pressure on each side of the diaphragm gives a direct measure of the pressure in the pumped vessel. Thus in contrast to the Bourdon-tube vacuum gauge, indications of the diaphragm gauge are indepedant of atmospheric pressure.

The bellows (capsule) vacuum gauge

In, this effect this type of gauge operates on the same principle as the diaphragm instrument. To extend the tip travel, the diaphragm is replaced by a bellows, a one piece expandible and collapsible member axially flexible. It is usually formed from thin seamless tube into a deeply folded or corrugated unit. Owing to higher flexibilty, the bellows vacuum gauge has a far higher sensitivity than diaphragm gauge.

3.5 THERMAL CONDUCTIVITY VACUUM GAUGES

Thermal conductivity gauges are widely used to measure pressures from 10^5 to 0.1 Pa.

For their operation, they depend on the relationship between the thermal conductivity of a gas and its pressure. At low pressures, when the mean free path of the gas molecules is longer than the mean distance between the heat source (usually a wire) and the enclosing bulb, the thermal conductivity of the gas is proportional to its pressure. At higher pressures, when the mean free path of the gas molecules is markedly shorter than the distance between the heat source and the bulb, the thermal conductivity of the gas is independent of its pressure. In the intermediate pressure range, heat transfer increases with rising pressure until it attains a constant value.

Of all modifications, two types of the thermal conductivity vacuum gauge are most commonly used. They are the Pirani gauge and the thermocouple gauge.

In its simplest form, the Pirani gauge is a glass or metal tube enclosing a wire stretched along the tube's axis and heated by passage of electric current (Fig.3.7). The energy fed to the wire, or the filament, is expended to heat the gas and to sustain the energy lost by radiation and conduction through the leads . At low pressures, the energy balance may be written as

$$I^2 R_f (1 + \alpha_f \Delta T) = c_f p \Delta T + \sigma_f (T^4 - T_a^4) + b_f \Delta T \qquad (.13)$$

41

where

c_jp ΔT =power (heat) transferred by the gas surrounding the filament to the bulb

p= gas pressure in the bulb

ΔT= T - T_a

T = filament temperature

T_a = ambient temperature

$\sigma_f(T^4$-$T_a^4)$= power dissipated by the radiation (in accord with the Stefan Boltzmann law of radiation)

$b - f\Delta$T =power (heat)withdrawn by conducting through the filament suspension and leads

I = filament current

R_f = filament resistance at T_a

α_f = temperature coefficient of resistance for the filament material

c_f, σ_f, b_f = proportionality factors

The unknown pressure, p, can be by eqn(.13):

$$p = \frac{(I^2 R_f(1 + \alpha_f \Delta T) - (b_f \Delta T)(\sigma_f)(T^4 - T_a^4)}{\sigma_f \Delta T} \qquad (.14)$$

Equation (.14) describes the calibration curve of the gauge bulb. A change in the pressure can be inferred from the changes in the filament current with T and $T - a$ held constant,or from changes in the filament temperature,

with the filament current held constant.

The Pirani gauge (constant-temperature operation)
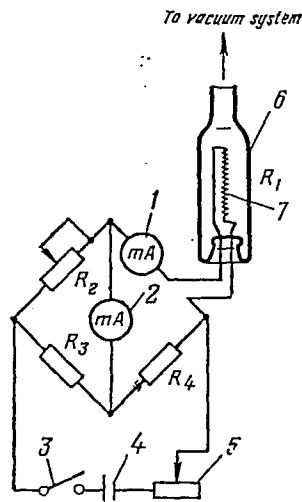
Fig 3.7 Pirani gauge

R_1—filament resistance; R_2—variable resistor; R_3—fixed resistor; R_4—fixed resistor; 1—milliammeter; 2—milliammeter; 3—switch; 4—battery; 5—rheostat; 6—steel tube; 7—tungsten filament

A likely arrangement of the Pirani gauge head and of the associated gauge circuit is shown in fig.2.7 . The gauge head is a steel tube 6 enclos-

43

ing a tungsten filament 7,stretched between two electrical leads-ins. The
gauge circuit is a Wheatstone bridge network formed by four resistances,
namely:

-R_1 which is the resistance of the filament having a high temperature coef-
ficient of resistance so that even a small change in the filament temperature
will bring about a marked change in R_1;

-R_2 which is a variable resistor fabricated of a material having a low coef-
ficient of resistance so that variations in temperature will not practically
affect value of R_2.
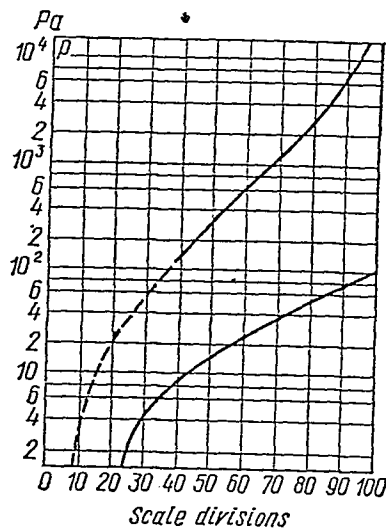
Fig 3.8 Calibration curves of
Pirani gauge in terms of air (Ref.14)

The upper solid curve corresponds to the
pressure range 4×10^3-92 Pa, the lower so-
lid curve corresponds to the pressure range
92-1 Pa

44

$-R_3$ and R_4 which are fixed resistors likewise having a low temperature coefficient of resistance and adjusted so that $R_3=R_4$.

As a rule, these resistors are wound with manganin or constantin wire. Pressure is measured by holding the filament at constant temperature . As the unknown pressure changes, the amount of heat withdrawn from filament also changes and so does the temperature. By adjusting the filament current I, the filament temperature is brought back to its original value, and the out of balance current involved is measured with an ammeter I, calibrated in units of pressure.

Calibration curves of a Pirani gauge are shown in Fig.3.8. As is seen, the range of the instrument extends from a few thousand pascals to 1 Pa.

Thermocouple gauge (constant current operation)

In sketch form the arrangement of a thermocouple gauge head and of its circuit is shown in Fig.3.9.

The gauge head is a glass or metal housing enclosing a platinum or nickel heating element 3, mounted on lead-ins or seals, and a Chromel-Copel or a Chromel-Alumel thermocouple 4, supported by another pair of lead-ins or seals.

Thermocouple and the heating element are welded together by a jumper 6. The heating element is fed with a current which can be adjusted with a rheostat 5 and measured with a milliammeter I. The hot junction of the thermocouple generates a thermo-emf whose value is indicated by a

millivoltmeter 2.
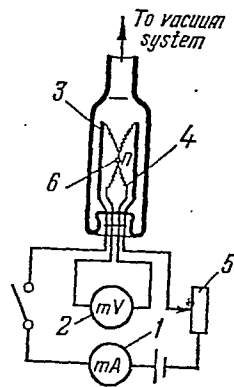
Fig 3.9 Thermocouple vacuum gauge

As long as the pressure in the pumped system remains equal to atmo-
spheric and the thermocouple bulb is fed with a specific filament current,I,

46

the millivoltmeter is reading zero very nearly. When the pressure in the pumped system decreases, the millivoltmeter moves up in thermo-emf, because a decreases in pressure leads to a decrease in the thermal conductivity of the gas and in consequence, to an increase in the temperature of the jumper.
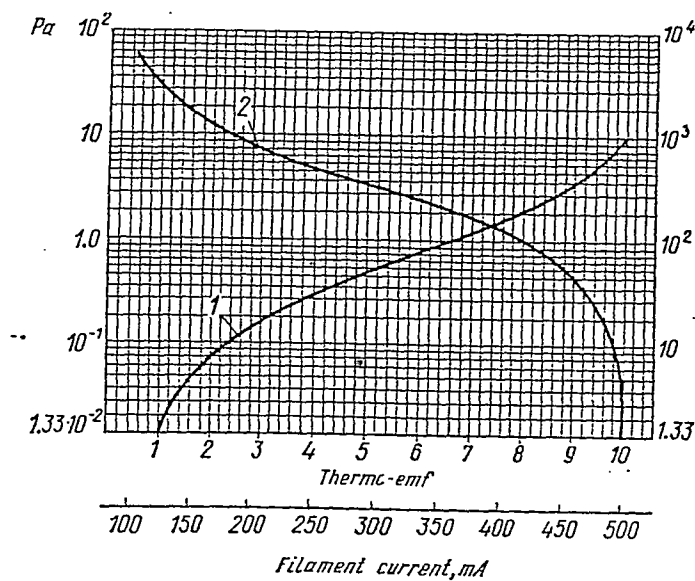
Fig 3.10 Calibration curves for a thermocouple vacuum gauge in terms of air (Ref.14)
1—for pressure measurement in the pressure range 6.6 × 10²–66 Pa; 2—for pressure measurement in the pressure range 66–1 × 10⁻¹ Pa

The accuracy of a thermocouple vacuum gauge depends to a considerable extent on the choice of the filament current value. It can be found prior to opening of a thermocouple bulb (if it is made of glass)or after the gauge head has been evacuated to p < 1.3×10^{-2} Pa. At that pressure, heat runaway from the heater with the gas is negligibly small, and practically all of the input power is radiated (about 63 percent) and conducted away

47

by the leads (about 37percent). The filament current is chosen such that the millivoltmeter reads the end-of- scale value. Therefore the milliammeter (the "filament current "scale) indicates the operating of the heater. Calibration curves in terms of air for a commercial thermocouple bulb are shown in the fig 3.10.

Merits and demerits of thermal conductivity vacuum gauges

Above all, thermal conductivity vacuum gauges are continuously reading simple in design and can measure the pressure of all gases and vapours. They are insensitive to vacuum failures and have practically unlimited service life. When contaminated by oil vapors, the gauge head can readily cleaned by washing in an organic solvent.If the gas involved caries too much oil or water vapor, it will be a good to install a refrigerated trap between the gauge head and the pumped system.

The demerits are that the thermal conductivity vacuum gauges are inferential (or indirectly reading) instruments and their calibration is different for different gases, being dependent on the thermal conductivity of the gases and the temperature accommodation of gas molecules on the heater. Another limitation is the variations in the filament current with time, so it has to be checked at regular intervals. The time lag of thermal conductivity gauges, although relatively small, also limits their performance.

3.6 HOT-CATHODE IONIZATION VACUUM GAUGES

Principle of operation

For their operation hot-cathodes (or thermionic) ionization vacuum gauges depend on the ionization of the gas by an electron stream. The ion current is a measure of pressure.

A cathode ionization gauge head (fig. 3.11) is essentially a triode tube. Its glass envelope I, encloses a ion collector 2, a highly positive grid 3 and a directly heated cathode 4 . The grid is held +200 V, and the cylindrical ion is collector at -50V. The grid is a coiled -coil filament made of tungsten wire 0.2mm in diameter.
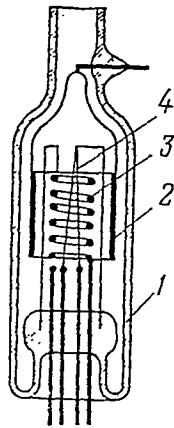
Fig 3.11   Thermionic
(hot-cathode) ionization
gauge

1—glass envelope;   *2*—ion collector;   *3*—anode;   *4*—cathode

Prior to use the gauge head is degassed by passing a current of 3A through the grid. The tungsten cathode emits electrons which move towards the collecting electrode. Some of the electrons pass through the grid and collecting electrode. Since the collector is negative to the cathode, electrons cannot strike the collector on the first pass. At a point in the space at zero potential the electrons come to a stop and set out on their travel in the reverse direction, towards the highly positive grid . Because of this, electrons can make as many as five oscillations about the grid before being collected. Colliding with gas molecules, the high velocity electrons ionize the gas within the envelope, and the positive ions so produced are collected by the collector which is negative towards the filament, thereby producing an ion current in the collector circuit.

As known from the experience, at sufficiently low pressures (ordinarily below 0.1Pa), the ratio of the ion current I_i, to the electron current I_e,is directly proportional to the gas pressure p_x, in the envelope given by

$$I_i/I_e = s_g p_x \qquad (.15)$$

Eqn(.15) is the basis for operation of a hot cathode ionization gauge head. The proportionality factor

$$s_g = (I_i/I_e)/p_x \qquad (.16)$$

50

is the sensitivity of the gauge head. Obviously,the sensitivity improves as the ratio I_i/I_e at a fixed p_x increases.

For the current to be definitively related to pressure, the electron current of the hot- cathode gauge is maintained constant. Then,

$$I_i = k_I p_x \qquad (.17)$$

where $k_I = s_g \times I_e$ defines the ion current per unit of pressure. It is sometimes termed the current sensitivity or current constant of a hot- cathode gauge.

The sensitivity of a gauge for individual gases is different than for air, but the linear relationship does hold. A comparison of the thermal-conductivity and hot- cathode ionization gauges in terms of their sensitivities for gases, air and nitrogen is given in Table below: On the basis of previous Eq. the pressure in the gauge bulb is given by

$$p_x = I_i/k_I \qquad (.18)$$

Or, in words to measure the pressure with a hot-cathode ionization gauge, it will suffice to measure the ion current at a given electron current and to divide it by the gauge constant.

A diagram of the gauge circuit is shown in the Fig.3.12 consisting of

(a) the cathode circuit 1, containing a power source and a rheostat 6, to adjust the temperature and, as a consequence, the emission of electrons;

51

(b)the grid circuit 2, which contains a power source and a meter 5, to measure the electron current;

(c) the collector circuit 3, containing a power source and a meter 4, to measure the ion current.

Hot-cathode ionization gauges for the medium vacuum range
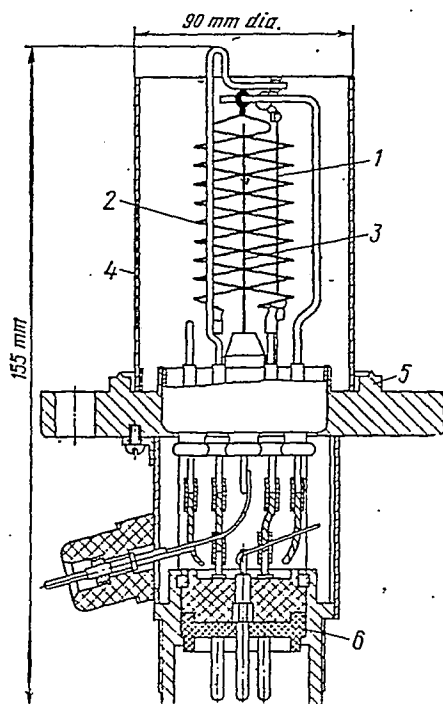
Fig 3.12 Hot-cathode ionization gauge
for very and ultra-high vacua (Ref. 14)

1—cathode; 2—anode grid; 3—ion collector;
4—shield; 5—flange; 6—base

The upper limit of hot-cathode ionization gauges is set by:

(1) the short service life of the usual tungsten thermionic cathode in the presence of reactive gases;

(2) the non linear relation between the ion current in the collector circuit and the gas pressure.

Theoretically, the upper limit is given by

$$p_{x.max} = 1/s_g \tag{.19}$$

From this eqn it follows that a hot cathode ionization gauges for high pressure should use a cathode which is highly resistant towards reactive gases and having a low sensitivity.

Hot cathode ionization gauges for high and ultra high vacuum.

The lower limit of pressure measured by hot cathode ionization gauges is set by spurious currents which are independent of the pressure. These above all include the current due to photoelectrons liberated by the collector electrode and the current due to ion-electron desorption from the grid. Photoelectrons emission takes place when the collector is exposed to soft X-rays which are produced at the grid by electron bombardment. The current due to the photo- electron emission is given by:

$$I_{ph} = k_{ph} I_e Z_a V_{a-k}^n \varphi \tag{.20}$$

where

$k_{ph}=$ proportionality factor

$I_e=$ electron current at the grid

$Z_a=$atomic number of the grid material

$V_{a-k}^n=$ anode(grid)to the cathode voltage

$\varphi=$solid angle subtended by the collector as viewed from the grid.

In a typical hot-cathode ionization gauge, spurious current due to photo-electrons emission has a value corresponding to a pressure of 5×10^{-7} Pa. In other words, such a gauge will measure a pressure of 5×10^{-6}Pa with a complementary error of 10 percent. Therefore, it is assumed that the lower limit, $p_{x.min}$ is set by $I_i=I_{ph}$ and, in accordance with eqns(.16)and(.17).

$$p_{x.min} = R_{ph}/s - g \qquad (.21)$$

where $s - g$ is the gauge constant and R_{ph} is the photo electron emission constant given by

$$R_{ph} = k_{ph}Z_aV_{a-k}^n\varphi \qquad (.22)$$

One way to minimize the spurious current constant is to reduce the solid angle φ. This is done by making the collector of a gauge for a very high vacuum as a fine filament or post.

There can be one more source of error in measuring low pressures. The electrons streaming towards the grid cause out gassing desorption of gas from its surface and ionize the gas in part. Together with the ions from the gas phase, the desorbed ions are intercepted by the collector and gives rise

54

to a spurious current in its circuit, thereby distorting the indication.

At pressure above 10^{-5} Pa, the effect of ion-electron desorption may be neglected. At lower pressures, it is important to suppress ion desorption current by giving the grid a thorough and sufficiently long warm up.

For a pressure upto 10^{-8} Pa, Commercial hot-cathode ionization gauges are pre dominantly built with a central (axial) collecting electrode,such as shown in the fig.3.13. The collector is arranged to lie along the axis of the grid 2,and made in the form of a fine tungsten post 0.1mm in diameter at the base and gradually tapering off towards the top.

The gauge has an expendable cathode I, which is located outside the grid. In operation, electrons oscillate on either side of the grid, and the collector intercepts only those ions which are formed inside it. The grid can be degassed by the electron bombardment or by a passage of current. In the latter case, the grid may be heated to 1100K.

The electrode structure is set up on a flange 5 directly inside the pumped vessel and surrounded by a grounded metal shield 4. The shield minimizes the effect of metal objects that may be present near and around the gauge and reduces the likely pick-up. At pressures above 10^{-2} Pa, the shield is dis- connected from the common return (ground) and is used instead of the grid which now acts as a collecting electrode.

Cold-Cathode Ionization gauges

Principle of operation

gauges in this class (also known as a sputter ion, Penning or Philips gauges) are capable of measuring both fairly high pressure around 10^2 Pa and very low pressures down to 10^{-10}Pa and lower.

Instead of a hot filament and electrons as in a thermionic ionization gauge, the gas in the bulb is now ionized by a self-maintained electrical discharge between two cold electrodes. This principle is illustrated in the simplified diagram of fig 3.14.

As seen, the bulb encloses two electrodes, namely a cathode which is in effect the metal envelope of the gauge 1, and anode in the form of a ring ,2. A magnetic field is setup and maintained along the axis of the anode at 0.05 to 0.2 T by a permanent magnet 4 in fig.3.14.

The anode is fed with a high positve voltage (2.5 -3.0 kV) via a current limiting resistor 3. When the pressure in the bulb is sufficiently low, a self maintained glow discharge takes place between the anode and cathode. For the discharge to take place it is necessary that at least one electron should turn up at the cathode. Acted upon jointly by electric and the magnetic fields the electron travels to the positive charged anode (collector) along a tremendously increased path. This enhances the probability for the electron to collide with and ionize the gas molecules. Such single electrons are present always, as they are readily produced by, say, cosmic rays. They

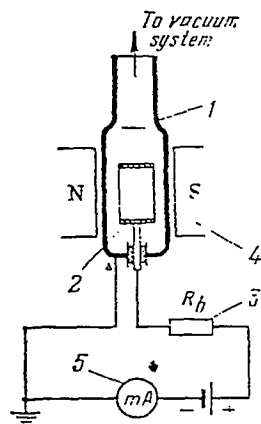give rise to (initiate) the ionization of the gas filling the gauge bulb.

Fig 3.14   Head and circuit of a sputter-ion gauge

The positive ions thus produced move towards the cathode and are neutralized them. As they have a substantial energy, they knock out of the cathode secondary electrons which, on moving towards the anode, also ionize the gas.

The ballast resistor automatically minimizes the difference in the voltage

between the electrodes at high pressures. In this way, it prevents the glow discharge from going over to an arc discharge in the inter electrode region. Between them, the current due to positive ions moving towards the cathode and the current due secondary electrons moving away from cathode add up numerically to the electron current in the (grid) circuit. Gas ionization results in a electrical discharge whose current is function of pressure over a sufficiently wide range. This relationship can be written as

$$I_d = \frac{V_{oc} - V_o}{R - b + k^{-1}p_x^{-n}} \tag{.23}$$

where

V_{oc} = open circuit voltage of the power source

V_o = minimum voltage between cathode and anode at the highest unknown pressure

R_b = external ballast resistor

k= sesitivity factor of the gauge

n=exponent (usually equal to 0.9 - 1.15)

Over a wide range of pressures, when $V_{oc}/I_d \gg R_b$,

$I_d = k_d \; p_x^n.$

where

$k_d = (V_{oc} - V_o)\text{k}.$

All cold cathode ionization gauges may be classed into two broad classes according to the relative alignment of the electrical magnetic field used. In some, the two fields are parallel to each other as in fig.3.15a. Others are

58

arranged to employ crossed electric and magnetic fields. Sometimes they

are further sub divided into magnetron types (as in fig. 3.15b)and inverted

magnetron types (as in fig 3.15c).

In gauges utilizing the Penning (cold cathode)discharge, no electron can

travel direct to the anode because of the applied magnetic field. In the

parallel-field arrangement(see fig 3.15a), electrons predominantly move to

and fro along the axis. In the magnetron type, electrons traverse a cycloid

(see fig 3.15b), whereas in the inverted-magnetron arrangement , they fol-

low a hypocycloid (see fig 3.15c).

Before they collide with gas molecules, electrons in a Penning gauge have

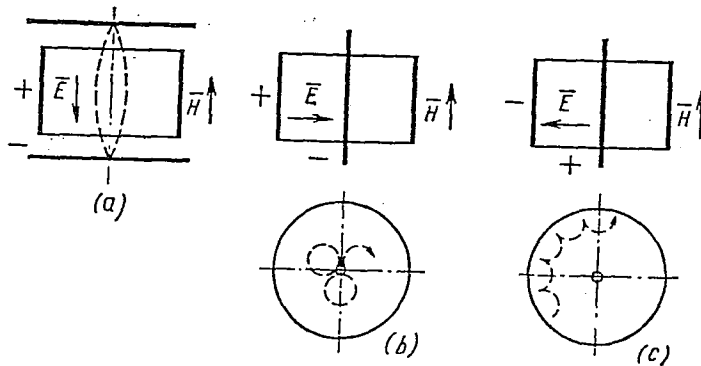travel huge distances running (in the high- vacuum range) into several kilo-

meters.

Fig 3.15
ron paths   Several forms of the sputter-ion gauge and the corresponding elect-

a—electric and magnetic fields mutually parallel; b—magnetron-type; c—inverted magnetron
type (electric and magnetic fields mutually perpendicular); E—electric field vector; H—mag-
netic field vector

59

CHAPTER IV

AVALANCHE IONIZATION MICRO PRESSURE GAUGE WITH B FIELD.

4-1 Introduction

As already discussed in chapter 1, the pressure in a chamber is an indication of the total number of molecules in that volume. A small imaginary volume of 1 cubic micron dimensions inside that chamber was considered. The molecules inside this volume was completely ionized and the ions collected on a separate electrode. The resulting ionization current when measured gave an accurate indication of the pressure inside the chamber.

In the following pages of this chapter, the ionization process, a device geometry which could accomplish this ionization, collect the ions and produce the ionization current has been discussed.

4-2 Influence of E and B fields on charged particles

The primary interaction between a particle of charge q and velocity v and magnetic field B is to produce a force F on the particle of magnitude F=Bqv. The direction of this force is perpendicular to both the magnetic field and the velocity. It is better expressed as

$$\mathbf{F} = q\mathbf{v} \times \mathbf{B} \tag{.1}$$

If the charged particle is also under the influence of an E field then the

force on the particle is additionally modified and is given by

$$\mathbf{F} = q(\mathbf{E} + \mathbf{v} \times \mathbf{B}) \tag{.2}$$

If the charged particle is an electron which is under the influence of an **E** field only, then it will be subjected to a force which will tend to make it move in a direction opposite to the direction of the **E** field. However, when the electron in addition to the **E** field is also subjected to a **B** field then the force on the electron is divided into two components. One due to the **E** field and other due to the **B** field. The force due to the **E** field subjects the electron to linear motion, while the **B** field force subjects the electron to circular motion. The linear and circular motions coupled together makes the electron move in a helical path. In otherwords when an electron moves in a helical path, its journey between two points that are in a straight line, is increased. The extent to which it is increased depends on the pitch and radius of the helix. The pitch and radius of the helix can be adjusted by suitably varying the **E** and **B** fields. The radius of the helix is given by

$$\frac{m_e(vsin\theta)^2}{r} = \mathbf{B}_e evsin\theta \tag{.3}$$

or

$$r = \frac{m_e vsin\theta}{\mathbf{B}e} \tag{.4}$$

Hence we see that the radius of the helix is independent of the **E** field and is inversely proportional to the **B** field.

The following is an analysis of Eq(.2) giving a relationship between the

motion of an electron and the direction of the E and B fields. Let us consider that the B field is applied in the Z direction and the E field is applied in the negative X direction. Initially, the electron is assumed to be under the influence of thermal energy. Hence a valid assumption is that it has velocity components in the X,Y and Z directions. The force on the electron due to the B field alone is

$$\mathbf{F} = q(v_x + v_y + v_z) \times \mathbf{B} = q(-v_x \mathbf{B}_z)\hat{a}_y + (v_y \mathbf{B}_z)\hat{a}_x) + 0 \qquad (.5)$$

The force on the electron due to the E field is given by

$$\mathbf{F_e} = -q\mathbf{E_x} \qquad (.6)$$

The total force on the electron is given by

$$\mathbf{F} = \mathbf{F_B} + \mathbf{F_e} \qquad (.7)$$

But since the force -qE_x approximately cancels the x components of the B field force F has only a negative component and its magnitude is given by -q$v_x B_z$. The trajectory of this electron as simulated by SIMION is shown in Fig(4.1).

As stated earlier the radius of the helical path is independent of the E field and is inversely proportional to the B field. However, the pitch of the helix is proportional to the ratio E/B. So, if the pitch is to be made very small, as small as $1A^\circ$, the B field must be very large compared to the E field. Since we cannot decrease the E field below a certain value due to reasons

63

Trajectory of electron under the
influence of E and B fields.
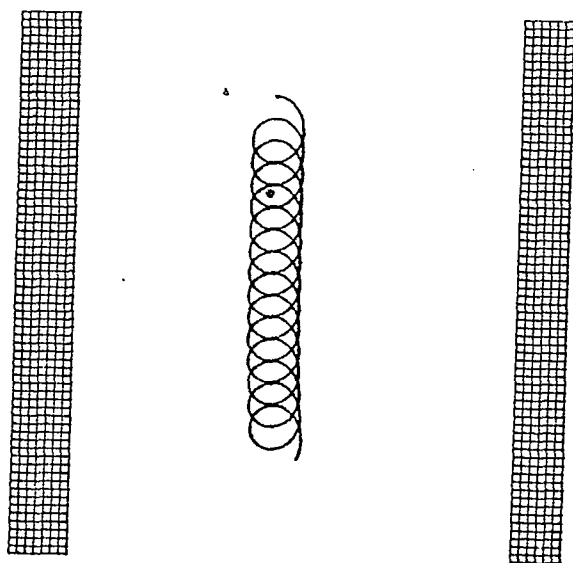

Fig (4.1)

discussed later in the chapter we are now only left with the B field which can be varied to obtain the desired pitch.

4-3 Ionization Process

Let us consider an electron travelling under the influence of an E and B fields. The pitch of the helix was adjusted(by suitably adjusting the ratio of E/B so that it is in the order of a few Angstroms. If this electron travels between two points that are in a straight line separate by a distance of 5 microns it would have in effect travelled a total distance of a few kilometers. During this enhanced path of the electron, the B field plays no role in increasing the kinetic energy of the electron. On the contrary the E field produces a force which helps the electron in increasing the kinetic energy. As a matter of fact the electron, only under the influence of the E field is subjected to a force which obeys the Newton's second law. This motion can be described by the equations of kinematics.

When the same electron is surrounded by a gas ambient like argon, oxygen, nitrogen or even air the electron will encounter collisions with these gas molecules. When the energy of the electron is greater than the ionization energy of the gas molecule at the instant of collision, ionization will result. For a typical gas molecule like xenon the ionization potential is 12.08eV. This means that the xenon gas molecule has to be struck by an electron having kinetic energy atleast equal to 12.08eV and that the electron itself should be accelerated through a potential of 12.08V, if it had started from

rest . A collision of an electron with a molecule produces two more charged particles; an ion and another electron. This may be represented as:

$$e + A \rightarrow A^+ + 2e^- \qquad (.8)$$

The direction of motion of the ion is in the direction of the E field and opposite to that of the electron. In a short time the total number of electrons would have increased to a very large proportion. The rate of increase is dependent on the total number of ionization that take place per unit time. As the population of electrons increases to several thousand times the population of unionized molecules, the probability of an ionization occuring is greatly enhanced. This probability also increases if the pitch is reduced and is comparable to the atomic radius of the molecule. This is called Avalanche ionization because the electrons needed for ionization is produced from the ionization process.

4-4 What is SIMION ?

SIMION is an electrostatic lens and design program originally developed at the Department at the Physics and Chemistry, Letrobe University in Australia. The SIMION PC/PS2 version, is an extensively revised version designed for highly interactive use on PC/PS2 class computers. Version 4.0 is the third major release of SIMION PC/PS2.

In SIMION, an electrostatic lens is defined as a 2-dimensional electrostatic potential array containing both electrode and non-electrode points. The

potential array is refined using over-relaxation methods allowing voltage contours and ion trajectories to be computed and plotted. Planar and cylindrical symmetry assumptions allow the 2-dimensional fields to support 3- dimensional ion trajectory calculations. Moreover, the user has the option of writing simple programs that can control field scale factors, dynamically adjust electrodes, define explicit 3- dimensional field function(e.g. quadpole) that are used in lieu of array fields in specified portions of the potential array, and much more!

SIMION PC/PS2 supports potential arrays up to 16000 double precision (64 bit) points. Speed enhancing features, include dynamically self-adjusting over- relaxation and presetting of voltage gradients to speed refining by up to a factor of 10. A fast adjust option, allows voltages in large arrays to be adjusted in seconds. Magnetic fields can be specified by the user for computing ion trajectories in many electrostatic and magnetic field environments.

Trajectory computations employ self-adjusting intergration intervals to reduce trajectory errors, and the contouring option automatically pick voltage contours for display by examining the electrodes. Neutralizing ions are also supported. Ion/neutral trajectories can originate outside the potential array, and focal points outside of the potential array are estimated to help reduce array sizes.

4-5 Device Geometry

67

The proposed device, to produce the avalanche ionization and to collect the resulting ions separately is shown in Fig(4.2).

In this device, there are four electrodes which are biased appropriately to achieve the desired effect. The actual ionization takes place between the two electrodes B and C, and in the region just above it where electrode B is grounded while C is biased to -50V. The reason for C to be biased to -50V is discussed in the following paragraph.

Assuming that this device is measuring pressure in a chamber containing xenon gas where minimum ionization energy of xenon is 12.08eV. Consider an electron starting from rest near ·C and moving towards B. Let the distance of separation between C and B be S. After the electron has travelled a distance of $S/3$ it would have acquired energy greater than the ionization energy of xenon and is capable of effective ionization. If an ionization has indeed occured, then the energy of the electron is reduced to zero. The electron again continues its journey towards C and for the same electron to produce the same effective ionization should travel through another distance of $S/3$. It can be concluded that this electron is capable of producing three effective ionizations during the course of its travel from C to B. A voltage of approximately 13V would have sufficed, to produce atleast one ionization. But this would have resulted in poor efficiency of the entire ionization process.

In this device the B field is applied in a direction perpendicular to the plane

of the paper. The trajectory of the electron and ion under the influence of these fields are shown. The value of the **B** field to produce the appropriate electron trajectory i.e. a helical path with the required radius and pitch was found to be around 10 Tesla(SIMION Simulation). In this case the radius of the helix was found to be 0.056 microns and the pitch was about $1.5A^0$ The electron tends to make a gradual drift towards electrode B ionizing molecules in its path. At the sametime the ions tend to move towards C. The **active volume** of the device may be defined as the region where the avalanche ionization occurs. In Fig(4.2) the active volume is between electrodes B and C including the volume directly above BC up to where the effects of the **E** field due to the voltages on B and C can be felt.

The ions produced in the active volume would normally tend to move towards C if A and D were not present. It is desirable to collect the the ions on a seperate electrode. The structure of the device became slightly complex to have this accomplished. In the figure the electrode D is biased at -100V and A is biased at 10V.The role of D is to attract the ions on to it by overcoming the electrostatic force of attraction between the ion and C. Electrode A enhances this effect and its role is more of a deflection plate than anything else. Fig 4.3 and 4.4 show the trajectory of the electrons and ions in the active volume of the ideal geometry respectively.

From simulation results it was concluded that a slight change in the geometry of A or a change in the voltage applied to A could changes the

Fig. 4.2

Geometry of optimized device showing
electrodes (black) and active volume (orange)

A
10 V

B
O'

C
-50 V

D
-100 V

1.1 μm
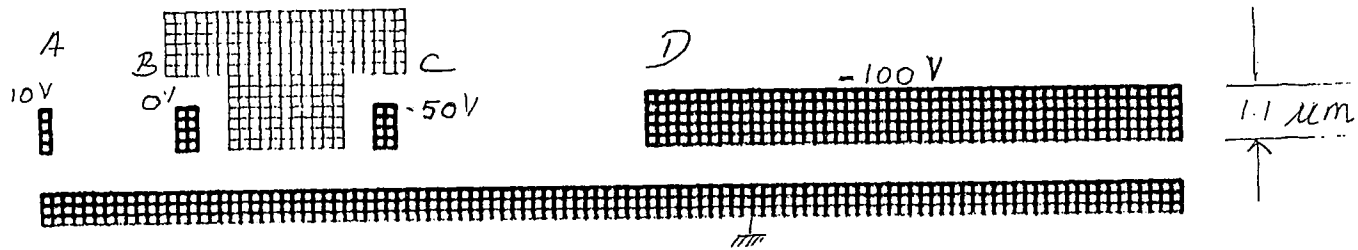
Fig. 4.3

Trajectory of electrons in the ideal device
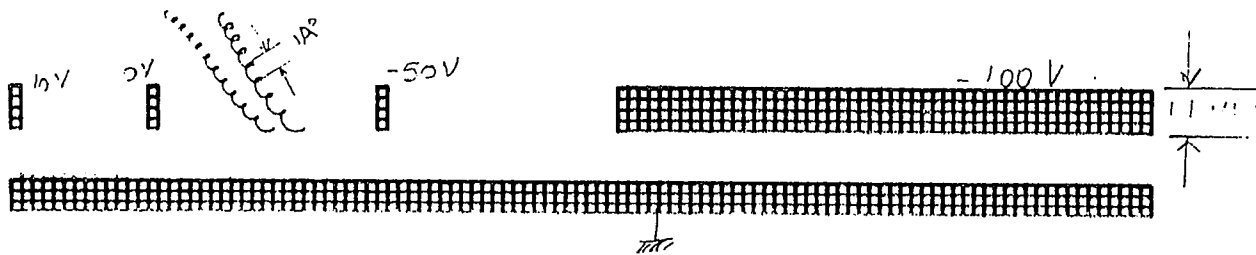
Fig. 4.4

Trajectory of ions in the ideal device

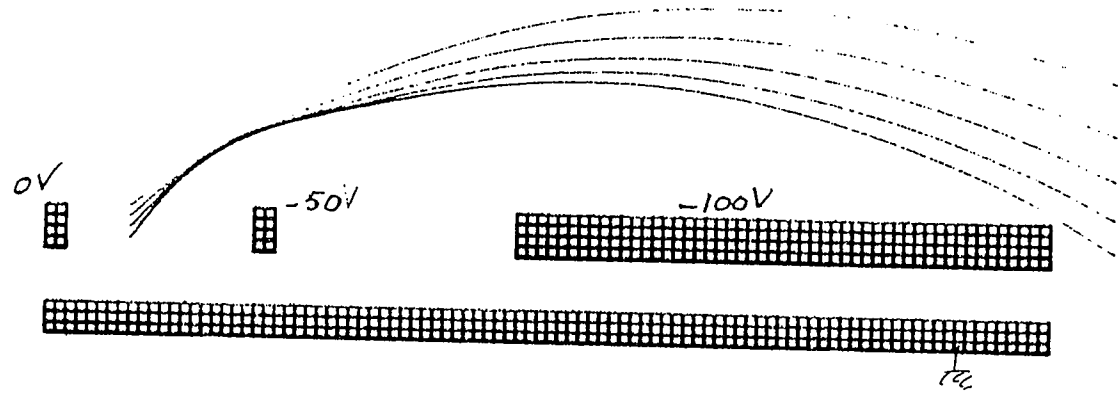10V   5V   50V   -100 V

1.1 μm
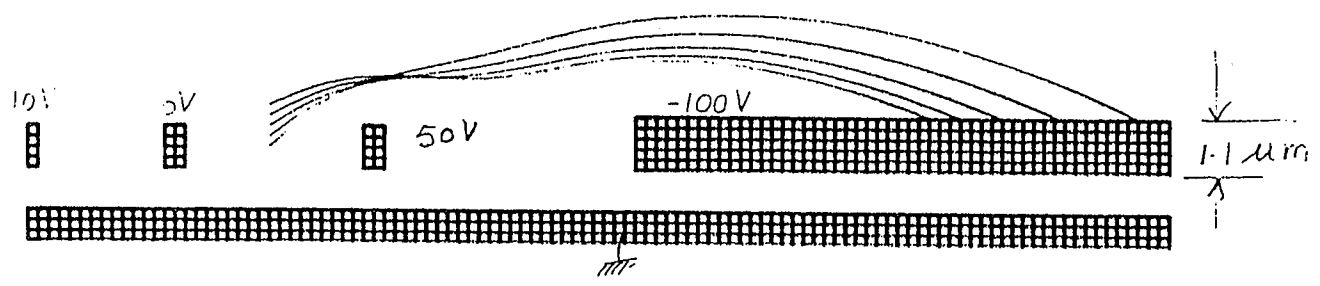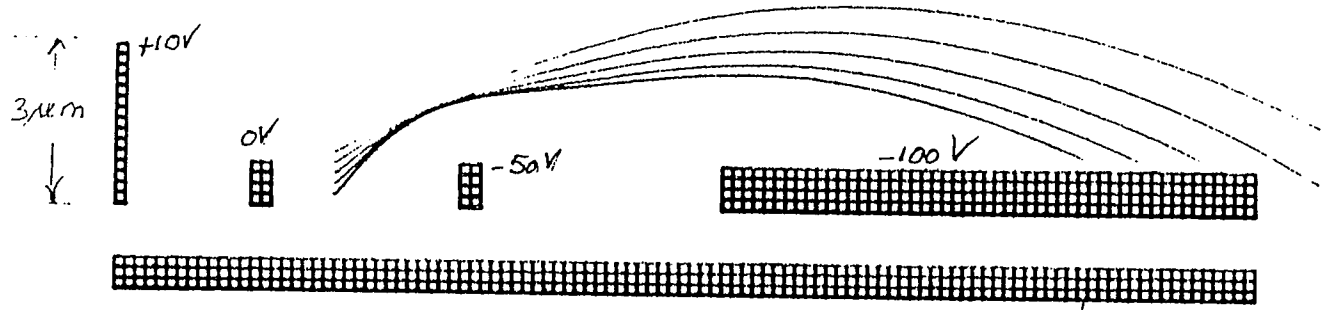
Trajectory of ions when geometry of
deflection electrode is changed

Fig. 4.5

Trajectories of ions without the
deflection electrode

Fig. 4.6

trajectory of the ion drastically. Figure(4.5) shows the variations in the ions trajectory due to the change in A's geometry and applied voltage.

4-5.2 Source for B Field

The source of steady magnetic field may be a permanent magnet an electric field changing linearly with time or a direct current. Our present relationships will concern the magnetic field produced by a differential dc element in the free space. It is assumed that this differential current element is a vanishingly small section of a current carrying filament conductor, where a filament conductor is is the limiting case of a cylindrical conductor of circular cross-section as this radius approaches zero. It is assumed that a current I is flowing in a differential vector length of a filament dL. The Biot-Savart law then states that at any point P the magnitude of the magnetic field intensity produced by a differential element is proportional to the product of the current, the magnitude of the differential length and the sine of the angle lying between the filament and a line connecting the filament to the point P where the field is desired. The magnitude of the magnetic field intensity is inversely proportional to the square of the distance from differential element to the point P. The direction of the magnetic intensity is normal to the plane containing the differential filament and the line drawn from the filament to the point P. Of the two possible normals, that one is to be chosen which is in the direction of progress of a right handed screw

turned through the smaller angle to the line from the n filament to P. The Biot Savart law may be written concisely as

$$dH = \frac{IdL \times a_r}{4\pi R^2} \qquad (.9)$$

$$B = \int_s \frac{\mu K \times a_r dS}{4\pi R^2} \qquad (.10)$$

$$B = \int_{vol} \frac{\mu J \times a_r dv}{4\pi R^2} \qquad (.11)$$

where K and J represent the surface and volume current densities. In this device, the B field is incorporated by means of a surface current which produces the desired B field. Though increasing the surface current could increase the B field, there is again a theoretical limit to the maximum current a conductor can carry. This is because at very high current densities electromigration (discussed later in this chapter) plays a predominant role which may lead to device failure. However the desired B fields can be achieved by means of high T_c conductivity which makes use of temperature dependence on magnetic fields. In this device the current is travelling in the X direction, the field point in the Y direction and the field is in the Z direction.

4-6 Fabrication of the Device

The geometry of the device having been discussed the next step is to consider the methods of fabricating the device. Depending on whether inclined or vertical sidewalls is needed a <100> or a <110> silicon wafer

75

is used respectively. The wafer is doped to the intrinsic level. The first

step is to oxidise the wafer. This oxide acts as a mask for etching of the

substrate to produce the geometry. The next step is to pattern the oxide. A

photoresist like PMMA is used. After this the substrate is etched. Some

etchants dissolve a given crystal plane much faster than other planes; this

results in orientation dependent etching.
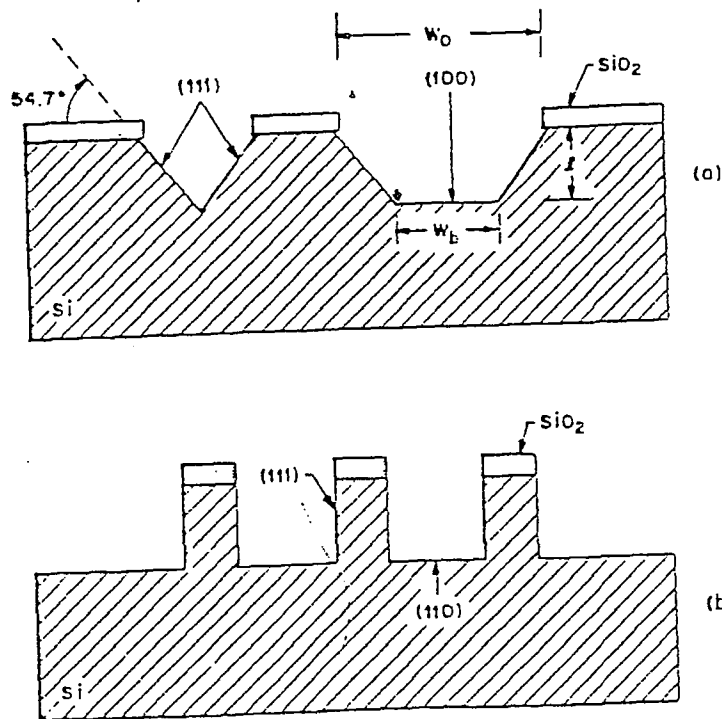
Orientation-dependent etching   (a) Through window patterns on $<100>$-oriented
silicon. (b) Through window patterns on $<110>$-oriented silicon

Fig 4.6

A commonly used orientation dependent etch for silicon consists of a mixture of KOH in water and isopropyl alcohol. The etch rate is $0.6\mu m/min$ for the (100)- plane, $0.1\mu m/min$ for the (110)- plane and only $0.006\mu m/min$ ($60A^0/min$) for the (111)-plane at about 80^0C; thus the ratio of the etch rates for the (100)-(110)- and (111)- planes is 100:16:1.

Orientation dependent etching of <100>- oriented silicon through a patterned SiO_2 mask creates precise V-shaped grooves, the edges being (111)-planes at an angle of 54.7^0 from the (100)-surfaces, as shown in the left of fig(4.6). If the window in the mask is sufficiently large or if the etching time is short, a U-shaped groove will be formed, as shown in the right of fig(4.6). The width of the bottom surface is given by

$$W_b = W_0 - 2lCot54.7^0 = W_0 - \sqrt{2}l \qquad (.12)$$

where W_0 is the width of the window on the wafer surface and l is the etched depth. If the <110>- oriented silicon is used, essentially straight walled groves with sides of (111)-planes can be formed, as shown in Fig(4.6). This property of orientation dependence in the etch rates is used to fabricate device structures with submicron feature length.Simulation results of the device fabricated on < 100 > substrate are shown in the figure(4.7).

Oxide is again grown over the entire substrate. The purpose of this oxide is to provide dielectric isolation between the metal that is to be deposited and the substrate. Since the properties of the oxide are not critical to the performance of the device wet oxidation is preferred to dry oxidation. An

77

Fig. 4.7

Geometry of device fabricated on a

100 substrate
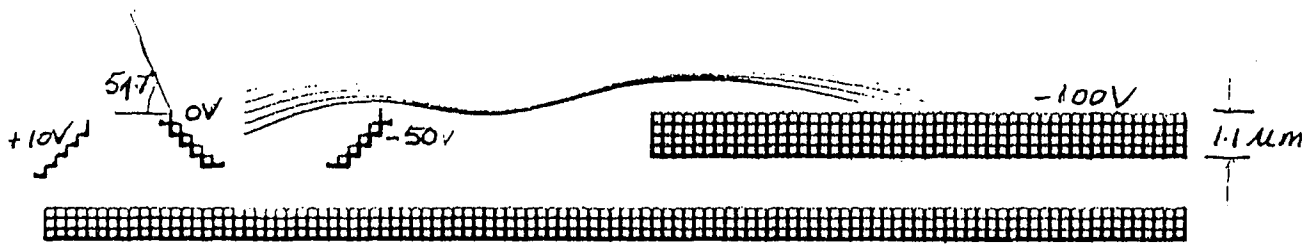
oxide thickness of $2\mu m$ would suffice.

The next step is to make a blanket deposition of metal over the oxide. Mmetallization may be carried out by two methods, either by sputtering or by vaporisation of a metal source. Aluminium is the preferred metal due to ease in processing and its lower resistivity. However the lower melting point of aluminium limits its use to processing steps after which no high temperature (normally greater than 450^0) operation is permitted. The resistivity of aluminium is 2.7-3.0 $\mu\omega$-cm and its melting point is 660^0C. It reacts with silicon at 250^0C and is stable on silicon upto about 240^0C. The metal is then patterned to define the electrodes A,B,C,D and the electrode which carries a current sheet (which acts as a source for the B field). Contact cuts are made on the respective electrodes to either bias them or collect the ionization current

4-6.2 Electromigration

Aluminium when carrying excessive currents suffers from electromigration. Electromigration can cause considerable material transport in metals. It occurs because of the enhanced and directional mobility of atoms caused by

(i) the direct influence of electric field and

(ii) the collision of electrons with atoms, which leads to momentum transfer. Thus, in devices using aluminum, failures caused by electromigration have been discussed. Aluminum is gathered in the direction of electron flow,

leading to a discontinuity in the conductor. This type of device failure seriously affects the reliability of the device.

The drift velocity v of migrating ions is given by

$$v = j\rho \frac{qz^*}{kT} D_0 e^{-\frac{Q}{kt}} \qquad (.13)$$

This equation is derived theoretically from the Einstien drift velocity equation.It has been modified for use in determining the relationship between the median time of failure(MTF) j and Q. MTF is the time, for a given testing condition, at which 50 percent of the testing sites will have failed. A general expression for MTF is

$$MTF \alpha j^{-n} e^{\frac{Q}{kT}} \qquad (.14)$$

In equation .13 and .14, j is the current density, n an exponent between 1 and 3, ρ is the film resistivity, qz^* the effective ion charge, k Boltzmann's constant, T the absolute temperature, D_0 the prexponential diffusivity and Q the diffusion activation energy.

Electromigration - induced failure is the most important mode of failure in aluminum lines. Most MTF measurements for a given current, are for MTF as a function of temperature and the linewidth of the conductor. The results are found to be strongly influenced by the method of deposition of the metal, the temperature of the substrate during deposition, the alloying element if any, the substrate type, the film thickness and the length of the conductor.

Addition of copper to aluminum considerably increases the electromigration resistance, which is also found to depend strongly on the method of deposition of the metal film, in addition to the linewidth.

The apparent superiority of Al-Cu alloys and e-gun evaporated metal or alloys is associated with the resulting preferred 111 textures and improved grain size distribution such as a bamboo structure. It is speculated that in addition to changing the structure the structure of the aluminum films, the addition of copper increases the electromigration resistance by enhancing the activation energy of the self diffusion of aluminum.

It has been shown that increasing the MTF first decreases with the length of the aluminum interconnect and then becomes independent of the length for all practical purposes. A current density threshold, which is found to be inversely proportional to the aluminum interconnect length exists, below which the mass transport due to electromigration stops. Thus, for a given current through the interconnect, the electromigration induced mass transport is higher in small interconnects. It has been suggested, the stress gradients in the film are the prime cause for this reverse mass transport and current density threshold.

4-7 A Method to increase Ionization Current

The device discussed above, can measure pressure only within certain ranges. The lower limit of this pressure range depends on the accuracy to measure very small ionization current which is of the order of sub-pico to femto amps. For example, when the pressure to be measured is of the order of 7.5×10^{-10} torr the ionization current, for an active volume of 5 cubic micron is 7.816×10^{-14} Amps. It becomes difficult to measure current of this order accurately. At high pressures, of the order of 1-10 torr the electrodes may be damaged due to sputtering from the ambient gas molecules. Hence, the pressure range over which the device can operate by picking up ionization current of sufficient magnitude and at sametime not suffer damage due to sputtering is specified as 10^{-4} to 10^{-7} torr. At 10^{-7} torr the ionization current is 7.83×10^{-11} amps. The magnitude of ionization current at this pressure can be increased by fabricating a number (about 100) of these devices on the same substrate and collecting the resulting ionization current from each individual device on one common electrode

CHAPTER V

Field Emission Micro Pressure Gauge

5-1 Introduction

The Avalanche ionization micropressure gauge discussed in the last chapter had a basic disadvantage and that is to produce a large magnetic field at room temperature. The B field is a critical parameter, since the efficiency of the ionization process to a great extent depends on the pitch of the helix. The pitch in turn is inversely proportional to the magnitude of the B field. Thus, the efficiency of the device suffers due the inability to produce high B fields.

In the field emission micropressure gauge the efficiency of ionization does not depend on the pitch of the helix, but it depends on the number of electrons emitted by the field emitter per unit time. Hence, the probability of an ionization increases as the number of electrons emitted by the field emitter increases.

5-2 Emission Properties

Field emission consists of tunnelling of electrons from a solid through the classically forbidden barrier region when the latter is deformed by the application of strong electrostatic field, $3\text{-}6 \times 10^7 \text{V/cm}$. In order to achieve these high fields at resonable voltages the cathode or emitter is etched to

a sharp point($<500A°$) so that a voltage of 100V will produce the desired field.

When an electron is emitted from a metal surface as a result of thermal excitation, it has to overcome a binding force (work function) of a few electron volts magnitude. Although this attraction potential is electrostatic in nature and therefore of long range ($V = 1/r$), it is reduced within angstrom from the crystal surface to a fraction of its value in the solid.
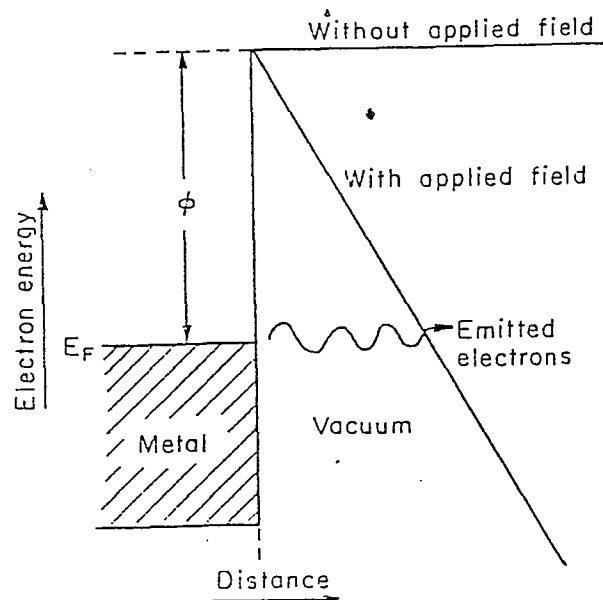
Potential-energy diagram for an electron at the metal surface in the absence and in the presence of an applied field.

Fig 5.1

Thus, electric fields of magnitude $E = 1V/A^0$ or, in more common emits $E = 10^8$ V/cm have to be overcome by electrons during the emission process. Therefore another method of producing electron emission from a solid surface is by the application of a large electric field of 10^7 to 10^8 V/cm normal to the surface.

The potential energy barrier,which has to be overcome by an electron for it to escape by the thermal excitation can be distorted this way and allows electron to "tunnel" through the emitter. A potential-energy diagram for an electron at a metal surface in the absence and in the presence of such an applied field is shown in Fig(5.1).Such an intense electric field can be obtained by applying a negative potential of 100V across a small cathode tip. The current density emitted from the tip is given by the Fowler-Nordheim equation,

$$j(A/cm^2) = 6.2 \times 10^6 (\phi E_F)^{1/2}/(\phi + E_F)(E^2)exp^{(-6.8 \times 10^7 \phi^{3/2}/E)} \qquad (.1)$$

where

E(V/cm) and ϕ(eV) are the field intensity and work function of the emitter respectively.

5.2 DEVICE GEOMETRY FOR AN OPTIMIZED DESIGN

The proposed device for the field emission micropressurre gauge is shown in the Fig(5.2). In this figure A is the substrate; B is the field emitter,with

C acting as a neutral electrode; D is the deflection electrode; F is another electrode when biased negatively serves as a collector to collect the ionized molecules.

The field emitter in this geometry is biased negatively while C is grounded. In this geometry, the electrons emerging out of the field emitter move towards C but do not get collected by C.This is due to the fact that the E field between D and F is strong enough to deflect the trajectory of the electron. This was done deliberately with the aim of increasing the active volume. Because, if all the electrons were collected by the anode then the active volume would be in its vicinty. The disadvantage of having any ions are produced in the active volume near C is because, when any ions are produced in the active volume the E field between the field emission cathode and C deflects the ions so strongly that it is able to attract them back to B.

This would finally damage the field emitter and at the same time reduce the ionization current to a very small fraction. Again a disadvantage occurs,the biasing anode and grounding the field emission cathode is that, if the ions are produced in the active volume , the electrostatic force of repulsion between the ions and the anode is so great that they are propelled directly upwards as in fig 5.2. A very large E field between D and F is required to deflect these ions. If such an E field is indeed used it could cause dielectric breakdown of the surrounding oxide.

The active volume of the device is shown in the figure. Any ionization produced here would retreat back to the field emission cathode resulting in sputtering of the field emission cathode.

Due to reasons discussed above it is necessary to bias the cathode negatively and ground point C. It is also necessary for substrate to be single crystal silicon with a minimum amount of grain boundaries. Again the resistivity of the single crystal silicon must be very high. The high resistivity is achieved by doping the silicon to the order of $2 \times 10^{12} atom/cm^3$. For this concentration the restitivity is approximately $2 \times 10^3 (\Omega - cm)$.The field emitter is grown on the substrate using epitaxial growth techniques.

In the next step oxide is grown in the region outside the field emitter. Selective metal deposition is made to define the anode of the field emitter.The thickness of the metal is about 0.1μm.
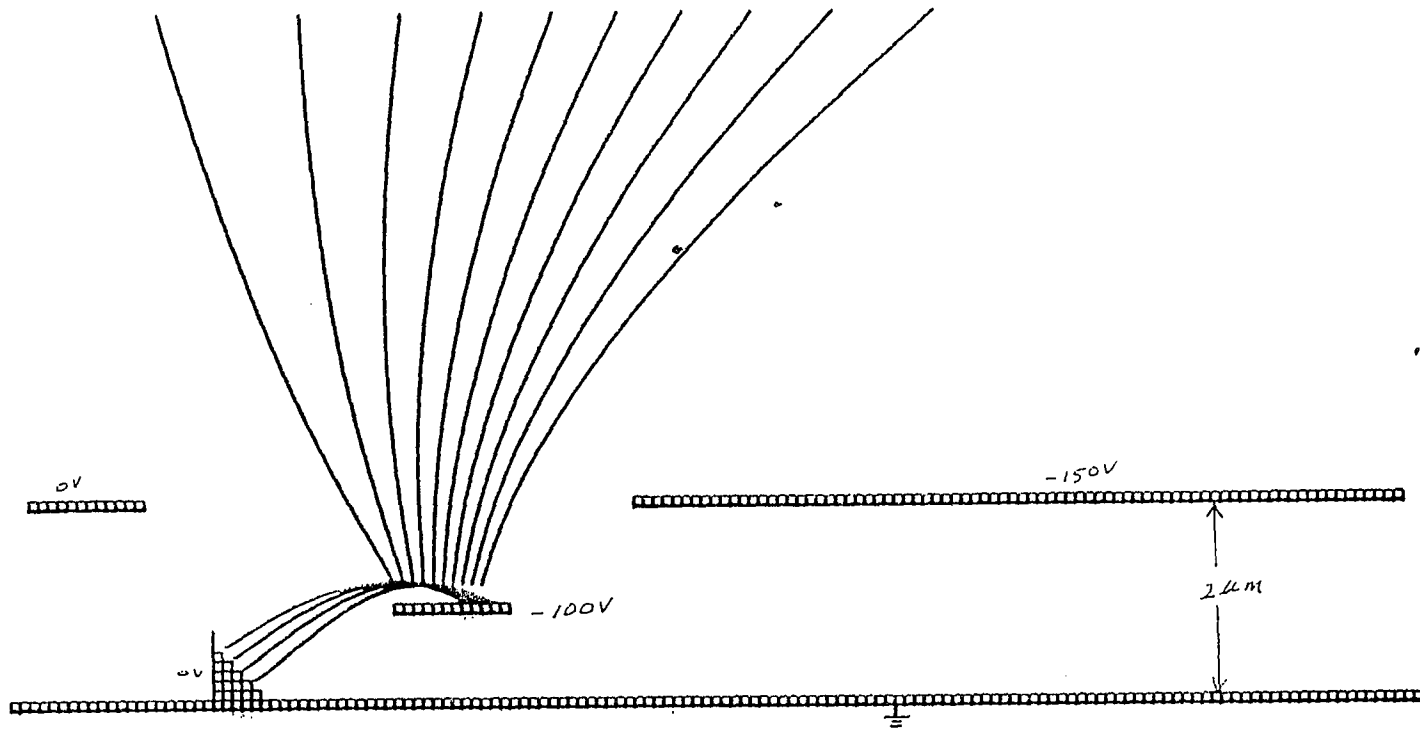
After this oxide is again grown in the region outside the field emitter and the anode .Again selective metal deposition is done to define the two electrodes D and F.

After A,C, D,F have been defined, B is now fabricated using step etching techniques to finally define the structure seen in the figure. The complete fabrication steps are tabulated in table 5.1. The physical processes are shown in fig. 5.3

Hence, when the field emitter is biassed at -100V this voltage is gradually dropped in the region between field emitter and the substrate. Simula-

Fig 5.2

Trajectory of ions when the field emitter is grounded

MICROMACHINING SEQUENCE·
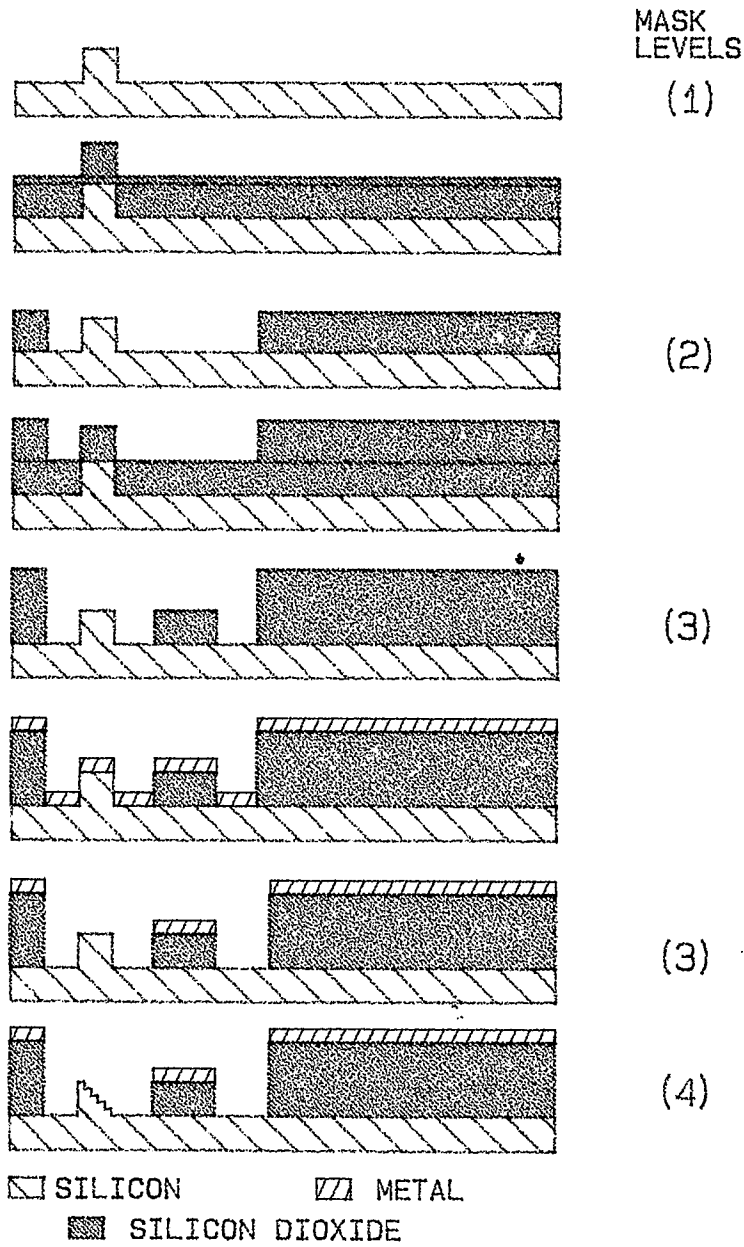# FOR DOUBLE LEVEL METALLIZATION

MASK
LEVELS

(1)

(2)

(3)

(3)

(4)

SILICON   METAL
SILICON DIOXIDE

FIG 5.3

Processing Sequence

for Double Level Metallization.

Process	Mask Levels	Discription
1	1	Etch the substrate to a depth of 1 micron to define the moat over which the field emitter is to be fabricated.
2	—	Deposit 1 micron thickness of silicon dioxide.
3	2	Pattern the oxide to define the deflection and collection electrode regions.
4	—	Deposit 1 micron thickness of oxide again.
5	3	Pattern the oxide to define the grid.
6	—	Deposit aluminum.
7	3	Pattern the aluminum to define all the electrodes.
8	4	Fabricate the field emitter.

table 5.1 :

90

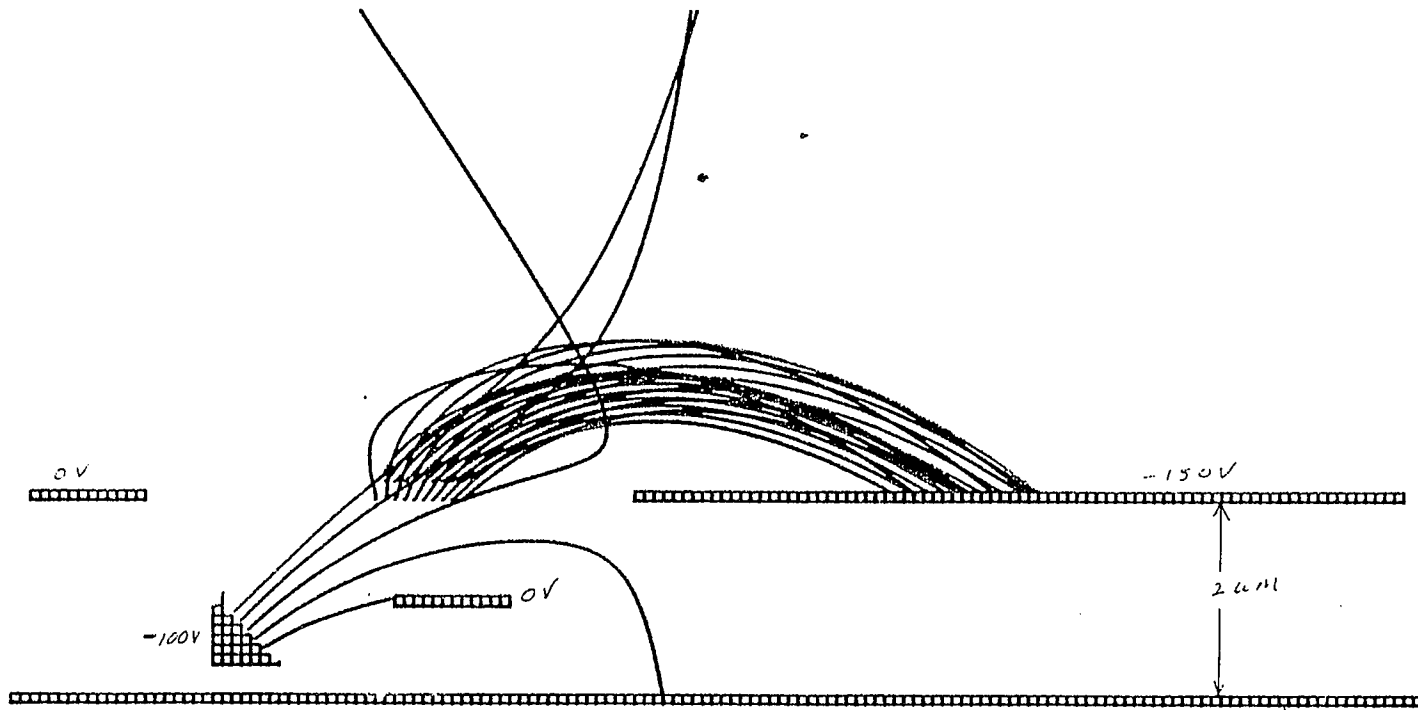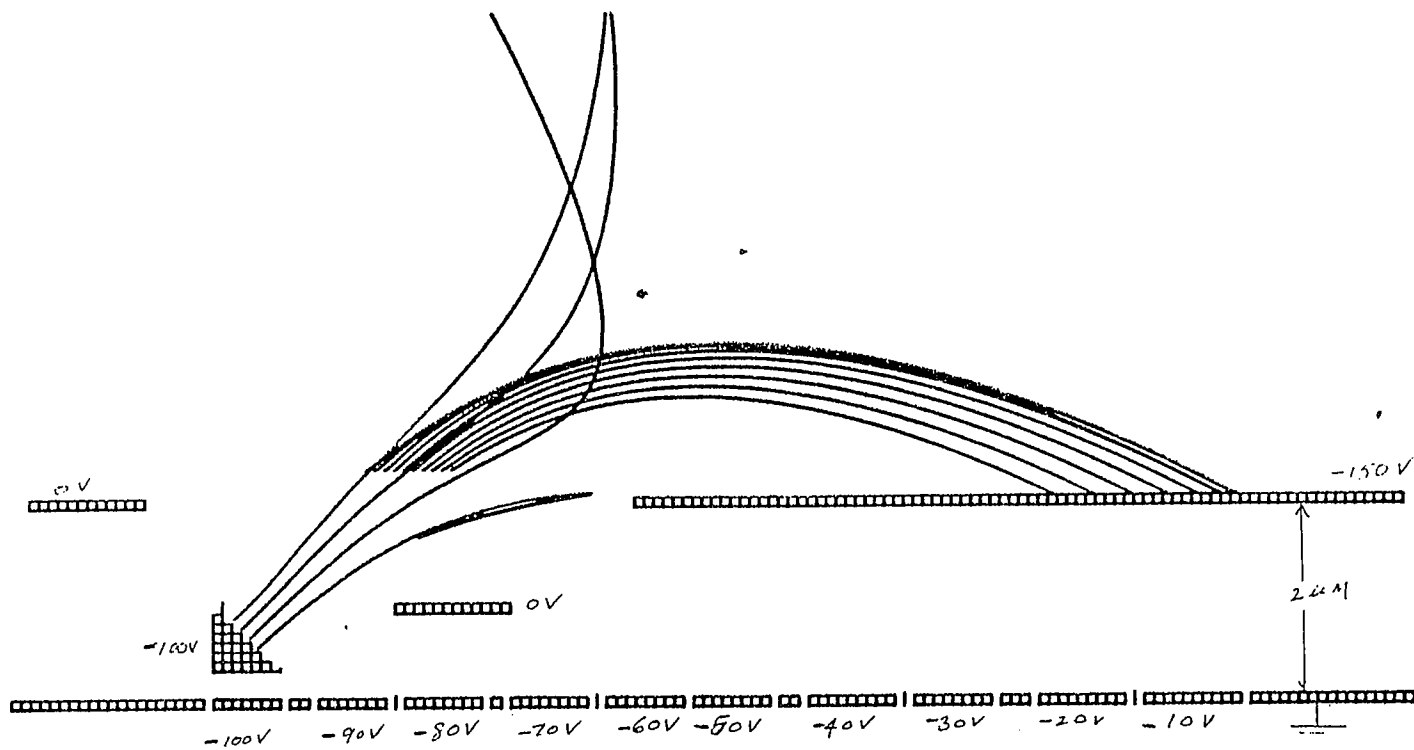Fig 5.4

Trajectory of electrons and ions in an
ideal geometry

Fig 5.5

Trajectory of ions showing the voltage across the substrate

0 V

−150 V

−100V

0 V

2 µM

−100V   −90V   −80V   −70V   −60V   −50V   −40V   −30V   −20V   −10 V

tion results showing the trajectory of the electrons with the field at -100V and the ground at zero volts with no second order effects is shown in the Fig (5.4). Also shown in the figure(5.5) is the potential drop across the substrate due to the high negative bias on the field emitter. It was seen that in the second case the active area increased slightly and the electrons trajectory was more favorable than the first.

5.3 SINGLE LEVEL METALLIZATION DESIGN

In the optimized design geometry, the number of masking levels are for too many, due to multilevel metallization. A simpler design,though not optimized has been simulated using single level metallization. Though, the fabrication of this device is far more simpler than the optimized design geometry, the major drawback of this geometry is that there is considerable decrease in the active volume leading to a smaller ionization current. For the single level metallization geometry shown in the figure(5.6)the active volume is about 1 cubic micron. Also the voltage on the collector electrode has to be increased considerably to deflect the ions so that a significant fraction of the ions may be collected. Due to this the existing E field is now increased approaching the dielectric breakdown of the oxide, thus requiring very pure oxide to be grown over the substrate.

5.4 LIFE OF THE FIELD EMITTER

Fig 5.6

Geometry of a single level
metallization device
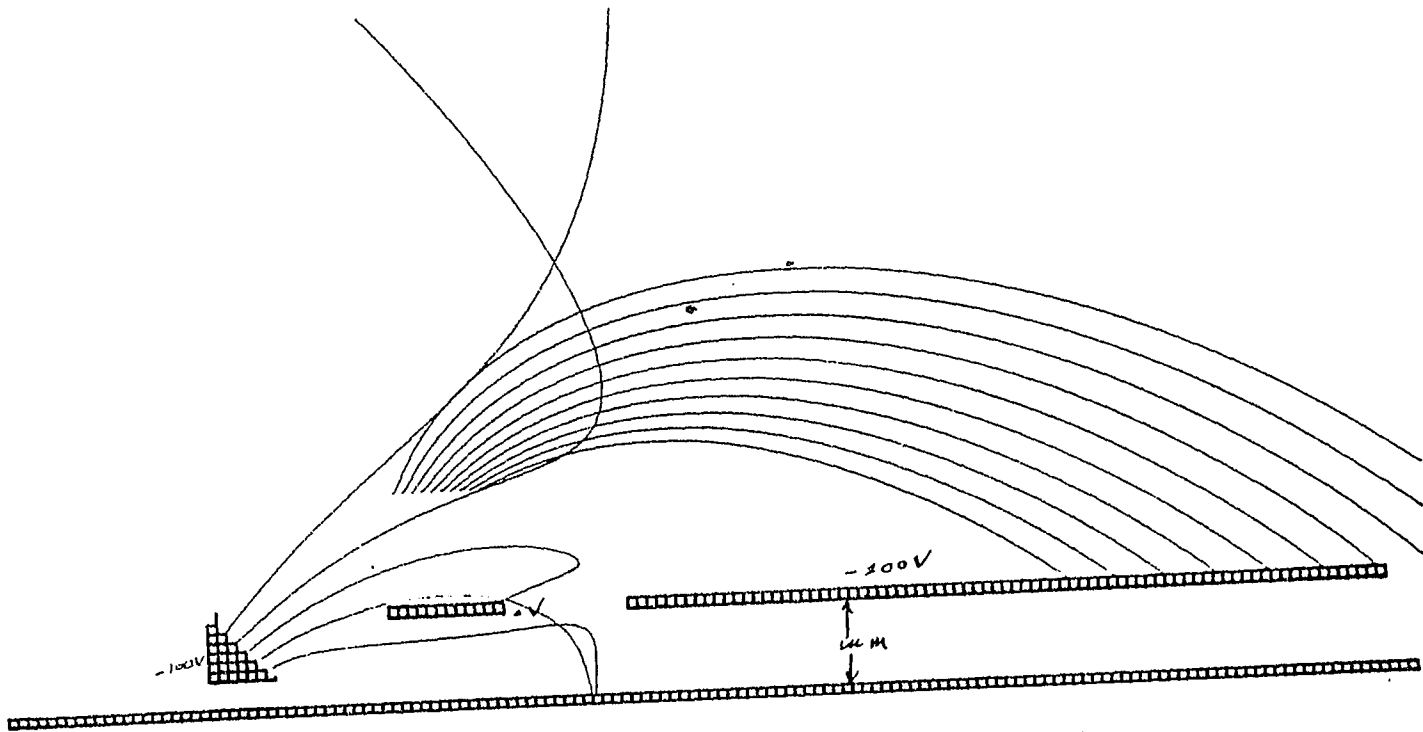
As was stated , earlier any ionization that takes place outside the active volume and near the field emission cathode,could be detrimental to the life of the cathode. When an ion strikes the emitting area, we may expect a sudden current fluctuation due to:

(1) Changes in the surface electric fields owing to the presence of the ion,

(2) changes in work function of the local surface as the ion is absorbed and subsequently described.

(3) Changes in the shape and work function of the local surface owing to the removal of a surface atom by sputtering.This will give permanent damage.

The time t_e taken to erode a single layer of atoms from an emission area is given by

$$t_e = \frac{\pi(ar_o)^2}{d^2 n_s} \qquad (.2)$$

where

d is the atomic spacing

a the emitting area

r_o cathode tip radius

n_s is the number of the atoms sputtered.

The life of the cathode is a function of pressure and is given by

$$L = \frac{2 \times 10^{-11}}{I_e P} \qquad (.3)$$

95

where

I_e is =the electron current .

P is the pressure inside the chamber

Hence, it can be easily seen that as the pressure inside the chamber decreases the lifetime increases. This sets the upper limit to the pressure that can be measured. The lower limit arises with our limitation to measure ionization current in the sub pico to finito amps accurately. It is projected that the device can measure pressure in the range between 10^{-4} to 10^{-7} torr accurately, with a field emission cathode.

MICROMACHINING SEQUENCE
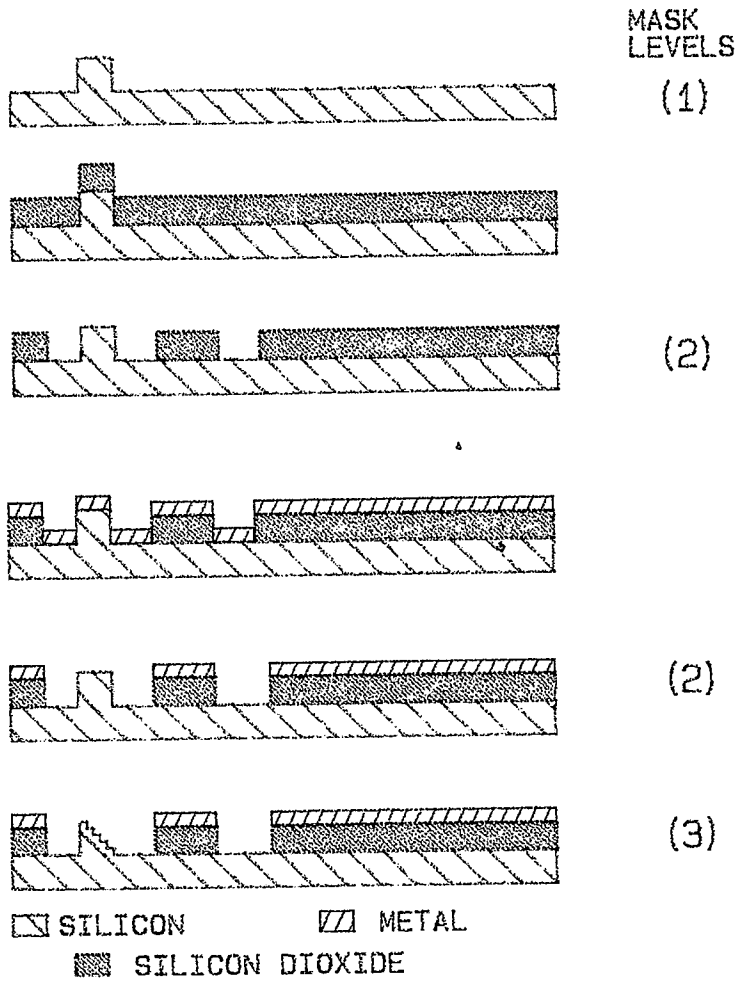# FOR SINGLE LEVEL METALLIZATION

MASK
LEVELS

(1)

(2)

(2)

(3)

◻ SILICON   ▨ METAL

▨ SILICON DIOXIDE

FIG 5.7

97

Processing Sequence

for Single Level Metallization

Process	Mask Levels	Description
1	1	Etch the substrate to a depth of 1 micron to define the mesa on which the field emitter will be fabricated.
2	—	Deposit 1 micron thickness of silicon dioxide.
3	2	Pattern the oxide to define the deflection, grid, and collection electrode regions.
4	—	Deposit aluminum.
5	2	Pattern the metal to define all the electrodes.
6	3	Fabricate the field emitter.

Table 5.1 c

CHAPTER VI

CONCLUSION AND SUMMARY

It has been shown that the two geometries discussed in the chapter 4 and chapter 5 are smaller than the existing ionization gauges by several orders. The simulation results from the SIMION are positive showing that this device will measure pressure accurately within the specified pressure range.

However both these devices have their own limitations. In the first geometry the entire device operation depends on the pitch of the helix. This in turn depends on the B field. Thus the performance depends on our ability to produce high B fields within this microstructure.

The second geometry which is more stable than the first does not incorporate a B field. This device also has an inherent disadvantage. The life of the field emission cathode may be reduced due to sputtering of ions due to field ionization. It was also shown that the life of the field emission cathode is inversely proportional to the pressure that can be measured.

Fabrication of both the devices is relatively simple. The fabrication of the field emitter requires the use of high resolution lithographic steps like ion beam lithography and submicron reactive ion etch, which by themselves are areas of extensive research. However a simple design (though not optimized) has been suggested.

REFERENCES

[1] Brian Chapman, *Glow Discharge Processes*. John Wiley and Sons,Inc: New York, 1980.

[2] S.C. Brown, *Introduction to Electrical Discharges in Gases*. Addison-Wesley: New York and London, 1967.

[3] D.Rapp and P.Englander-Golden, *Journal of Chemical Physics*. 43,4: 1464, 1965.

[4] B.L. Schran, F.J. de Heer, M.J. Van der Wiel and J. Kistemaker, *Physica*. 31: 94, 1965.

[5] L.E. Beam, *Anisotropic Etching in Silicon*. IEEE Trans. Electron devices: ED-25,1185, 1978.

[6] C.L. Hemenway, R.W. Henry and M.Caulton, *Physical Electronics*. Wiley: New York and London, 1967.

[7] S.C. Arney and N.C. MacDonald, *Journal of Vacuum Science and Technology*. Vol. B:6: PP 341-345, 1988.

[8] C.A. Spindt, I.Brodie, L.Humprey and E.R. Westerberg, *Journal of Applied Physics*. Volume 47: 5248, 1976.

[9] I.Brodie, *International Journal of Electron*. Volume 38: 541, 1975.

[10] I.Brodie, *Journal of Applied Physics*. Vol 35: 2324, 1964.

[11] R.Gomer, *Field Emission and Field Ionization*. Harvard University Press: Cambridge,Mass., 1961.

[12] S.M.Sze, *Semiconductor Devices, Physics and Technology*. John Wiley and Sons: New York, 1985.

[13] R.B. Marcus, R.Soave and H.F. Gray, *The First International Vacuum Microelectronic Conference.* : , 1988.

[14] A.Pipko, V.Pliskovsky, B.Korolev and V.Kuznetsev, *Fundamentals of Vacuum Techniques*. Mir Publishers: Moscow, 1981.

[15] R.H.Fowler and L.W. Nordheim, *Proc. Royal Scociety of London*. A 119: 173, 1928.